2017

Functional stability of HIV-1 envelope trimer affects accessibility to broadly neutralizing antibodies at its apex

Syna Kuriakose Gift
Military HIV Research Program

Daniel P. Leaman
The Scripps Research Institute

Lei Zhang
The Scripps Research Institute

Arthur S. Kim
Washington University School of Medicine in St. Louis

Michael B. Zwick
The Scripps Research Institute

AMERICAN SOCIETY FOR MICROBIOLOGY | Journal of Virology®

VACCINES AND ANTIVIRAL AGENTS

Functional Stability of HIV-1 Envelope Trimer Affects Accessibility to Broadly Neutralizing Antibodies at Its Apex

Syna Kuriakose Gift,* Daniel P. Leaman, Lei Zhang, Arthur S. Kim,* Michael B. Zwick

Department of Immunology and Microbial Science, The Scripps Research Institute, La Jolla, California, USA

ABSTRACT The trimeric envelope glycoprotein spike (Env) of HIV-1 is the target of vaccine development to elicit broadly neutralizing antibodies (bnAbs). Env trimer instability and heterogeneity in principle make subunit interfaces inconsistent targets for the immune response. Here, we investigate how functional stability of Env relates to neutralization sensitivity to V2 bnAbs and V3 crown antibodies that engage subunit interfaces upon binding to unliganded Env. Env heterogeneity was inferred when antibodies neutralized a mutant Env with a plateau of less than 100% neutralization. A statistically significant correlation was found between the stability of mutant Envs and the MPN of V2 bnAb, PG9, as well as an inverse correlation between stability of Env and neutralization by V3 crown antibody, 447-52D. A number of Env-stabilizing mutations and V2 bnAb-enhancing mutations were identified in Env, but they did not always overlap, indicating distinct requirements of functional stabilization versus antibody recognition. Blocking complex glycosylation of Env affected V2 bnAb recognition, as previously described, but also notably increased functional stability of Env. This study shows how instability and heterogeneity affect antibody sensitivity of HIV-1 Env, which is relevant to vaccine design involving its dynamic apex.

IMPORTANCE The Env trimer is the only viral protein on the surface of HIV-1 and is the target of neutralizing antibodies that reduce viral infectivity. Quaternary epitopes at the apex of the spike are recognized by some of the most potent and broadly neutralizing antibodies to date. Being that their glycan-protein hybrid epitopes are at subunit interfaces, the resulting heterogeneity can lead to partial neutralization. Here, we screened for mutations in Env that allowed for complete neutralization by the bnAbs. We found that when mutations outside V2 increased V2 bnAb recognition, they often also increased Env stability-of-function and decreased binding by narrowly neutralizing antibodies to the V3 crown. Three mutations together increased neutralization by V2 bnAb and eliminated binding by V3 crown antibodies. These results may aid the design of immunogens that elicit antibodies to the trimer apex.

KEYWORDS envelope, gp120, gp41, human immunodeficiency virus, neutralizing antibodies, protein stability, vaccines

A major goal of HIV-1 vaccine design is to elicit broadly neutralizing antibodies (bnAbs) that can protect against infection (1–3). The HIV-1 envelope glycoprotein (Env) spike tends to elicit B cell responses to variable regions and not to more conserved sites that are relatively hindered by adjacent glycosylation (2, 4–6). "Well-ordered" soluble Env trimers (e.g., SOSIP and NFL gp140s) have been developed to mimic the Env spike, which is comprised of three surface subunits (gp120) and three transmembrane subunits (gp41) (3, 7–10). These soluble trimers display desirable quaternary epitopes of various bnAbs, but how well they mimic native epitopes is not

Received 14 July 2017 **Accepted** 29 September 2017

Accepted manuscript posted online 4 October 2017

Citation Gift SK, Leaman DP, Zhang L, Kim AS, Zwick MB. 2017. Functional stability of HIV-1 envelope trimer affects accessibility to broadly neutralizing antibodies at its apex. J Virol 91:e01216-17. https://doi.org/10.1128/JVI.01216-17.

Editor Viviana Simon, Icahn School of Medicine at Mount Sinai

Address correspondence to Michael B. Zwick, zwick@scripps.edu.

* Present address: Syna Kuriakose Gift, Henry M. Jackson Foundation for the Advancement of Military Medicine, Military HIV Research Program, Bethesda, Maryland, USA; Arthur S. Kim, Department of Molecular Microbiology, Washington University School of Medicine, St. Louis, Missouri, USA.

S.K.G. and D.P.L. contributed equally to this article.

fully understood. In principle at least, the formation (and disruption) of quaternary epitopes relate to the stability of the Env trimer. Determining the potency, affinity and completeness of binding of antibodies to native Env, particularly to the V2 and V3 domains at its apex, might be crucial for vaccine design, since some studies have associated these regions with vaccine protection (11–13).

bnAbs against V2 derive from HIV-1-infected donors and are sensitive to Env trimeric structure; these bnAbs include PG9 and PG16 (14), PGT141-145 (15), VRC256.01-08 (16), and PGDM1400 (17), the latter being a potent variant in the PGT145 lineage. V2 bnAbs bind one-per-spike to a single β-strand "C" and N-linked glycan at position 160 while avoiding adjacent variability in V1V2 (4, 14, 15, 17–24). V2 bnAbs typically have long tyrosine-sulfated CDR H3s that interact with positively charged lysine residues in the C strand, including K168, K169, and K171 (21, 25, 26), but glycans proximal to N160 can also influence binding and neutralization (27, 28). V2 bnAb CH01 neutralizes a modest number (i.e., 48%) of tier 2 isolates and shows preference for trimmed man5 glycan at positions 156 and 160 on V2 (22). Kifunensine treatment of producer cells generates Env with untrimmed glycans (e.g., man9) that typically abrogates binding and neutralization by V2 bnAbs due to poor accommodation of man9 in their antigen-combining sites (15, 28–30).

Beneath V2 on Env lays V3, with its crown pointing inward toward the trifold axis of the spike (8). The exposure of the V3 crown on the trimer depends directly on its interaction with adjacent residues in gp120 (31). The crown is accessible to "tier 1" neutralizing antibodies, including 447-52D, F425-B4e8, and 19b, which typically cannot neutralize "tier 2" primary isolates due in part to masking of V3 by V1V2 on the resting spike (32). V3 extends outward from the crown to a conserved and exposed glycan at N332, which is a target of highly potent bnAbs including PGT121-122, PGT126, and PGT128 (15, 33, 34). Env trimers that occlude the V3 crown but stabilize the N332 supersite are of interest as immunogens (35–37).

Heterogeneity in Env is not uncommon (5). Glycosylation seems to be the dominant cause, which on V2 and gp41 can be relatively complex and variable (4, 38–41), but other factors that affect protein folding might also contribute. Env microheterogeneity may cause nonsigmoidal inhibition curves with HIV-1 and less than 100% maximum percent neutralization (MPN). Atypical neutralization curves have been associated mostly with bnAbs to V2, membrane-proximal external region (MPER) and the gp41 interface (5, 42, 43). Because antibody binding to these regions perturbs trimer symmetry (24, 43), preexisting heterogeneity in Env may affect antibody binding on a molecule-by-molecule basis by facilitating or resisting formation of the antibody-trimer complex.

We reported previously on a clade B Env trimer that was stabilized using directed evolution (44). We discovered that the stabilized Env, termed Comb-mut, was incompletely neutralized by V2 antibodies PG9 and PG16 and showed a tier 2-like resistance to narrow CD4 binding site (CD4bs) antibodies. In contrast, its labile Env counterpart, ADA, was relatively neutralization sensitive (tier 1-like). To determine the relationship between stability, heterogeneity and neutralization sensitivity at the apex of Env, we screened mutants of ADA and Comb-mut in assays for functional stability of Env and MPN of PG9, and a correlation was found between the two traits. Env stability of function also correlated inversely with the neutralization by V3 crown antibodies. A number of trimer stabilizing mutants were identified, and select mutant spikes showed relatively homogeneous neutralization by V2 bnAbs and relative occlusion of the V3 crown. The results accord with structural models of Env and inform the design of homogeneous HIV-1 trimer-based vaccines.

RESULTS

Neutralization of HIV-1 Env mutants by PG9 and V3 antibodies. Comb-mut is a mutant of HIV-1 ADA containing eight stabilizing mutations in Env (i.e., I535M, L543Q, K574R, H625N, T626M, S649A, N142S, and an N139/I140 deletion) that evolved during adaption of ADA to treatment with heat and GuHCl (44). Comb-mut was shown

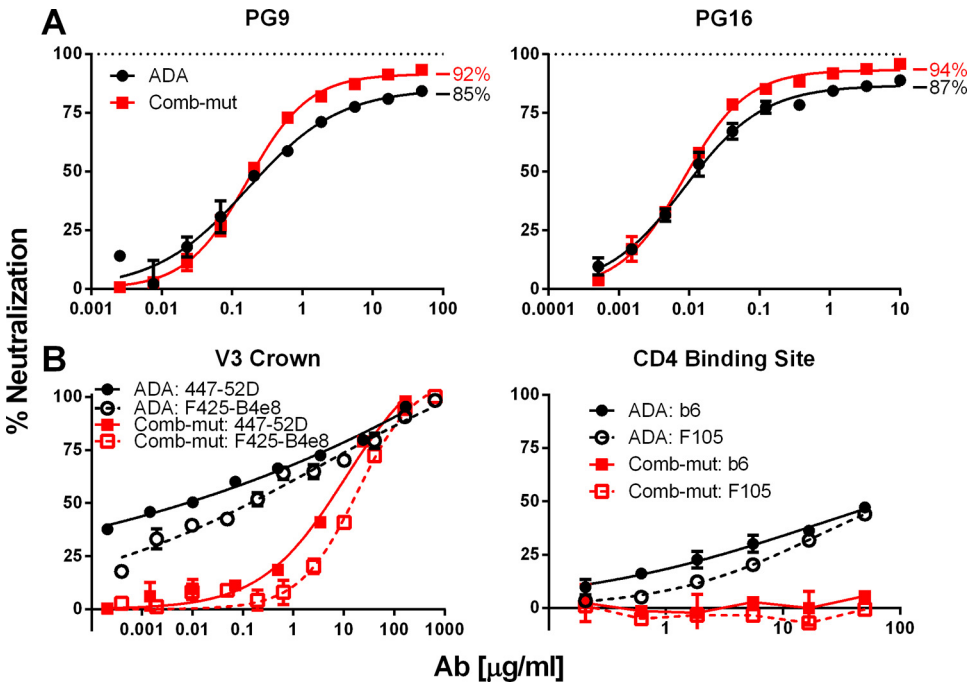

FIG 1 Neutralization of ADA and Comb-mut by V2 bnAbs, V3 crown antibodies, and CD4bs non-bnAbs. HIV-1 ADA and Comb-mut virions were tested in neutralization assays against the V2 bnAbs PG9 and PG16 (A) and the V3 crown antibodies 447-52D and F425-B4e8 and the CD4 binding site (CD4bs) non-bnAbs b6 and F105 (B). In panel A, the maximum percent neutralization (MPN) for each virus-antibody pair is noted.

previously to be more thermostable than a broad panel of tier 1 and tier 2 isolates (44, 45). In neutralization assays with PG9 and PG16, Comb-mut showed higher MPN values compared to ADA, but both viruses remained partially neutralized (i.e., 92 and 94% for Comb-mut versus 85 and 87% for ADA, respectively; Fig. 1A). The slopes of neutralization curves of PG9 and PG16 against Comb-mut were also steeper than with ADA, which suggests that Comb-mut trimers may be more homogeneous and uniformly recognized. In neutralization assays with V3 antibodies 447-52D and F425-B4e8, as well as the CD4bs "non-bnAbs" b6 and F105, we found that ADA was neutralized with shallow dose-response curves, although 100% neutralization was reached at high concentrations of V3 antibodies (Fig. 1B). Comb-mut was resistant to F105, b6, and V3 crown antibodies 19b and 39F (data not shown) but was modestly sensitive to F425-B4e8 and 447-52D. However, 447-52D neutralized ADA (50% inhibitory concentration [IC_{50}] = 0.05 μg/ml) ~100-fold more potently than Comb-mut. The neutralization curves with Comb-mut had the expected sigmoidal shape but were shallow with ADA (Hill slopes of 0.87 and 0.18, respectively). These results indicated that on Comb-mut epitopes of most non-bnAbs were relatively occluded and V2 bnAb epitopes were retained. We sought to investigate how V3 crown exposure and V2 heterogeneity in Comb-mut and ADA relate to functional stability of Env and to identify functional Env with improved V2 bnAb recognition and with V3 occluded.

Mutations that enhance neutralization of HIV-1 by PG9. To gain insight into V2 exposure on ADA and Comb-mut, we generated a mutant Env panel to be screened for sensitivity to PG9. Mutations in or near to the PG9-binding site were chosen in part based on sequence alignment of ADA, Env consensus M (ConS), as well as clade A and C stable Env trimers, BG505 and 16055, respectively, the latter of which exhibit 100% MPNs against PG9 and PG16 (Fig. 2). We also tested a variety of mutations outside of V1V2, including N-glycosylation knockouts, mutations that caused resistance to entry inhibitors PF-68742 (46) and 5P12-RANTES (47), as well as others which had been described or suspected to affect Env trimerization, as cited in Table 1 and discussed further below.

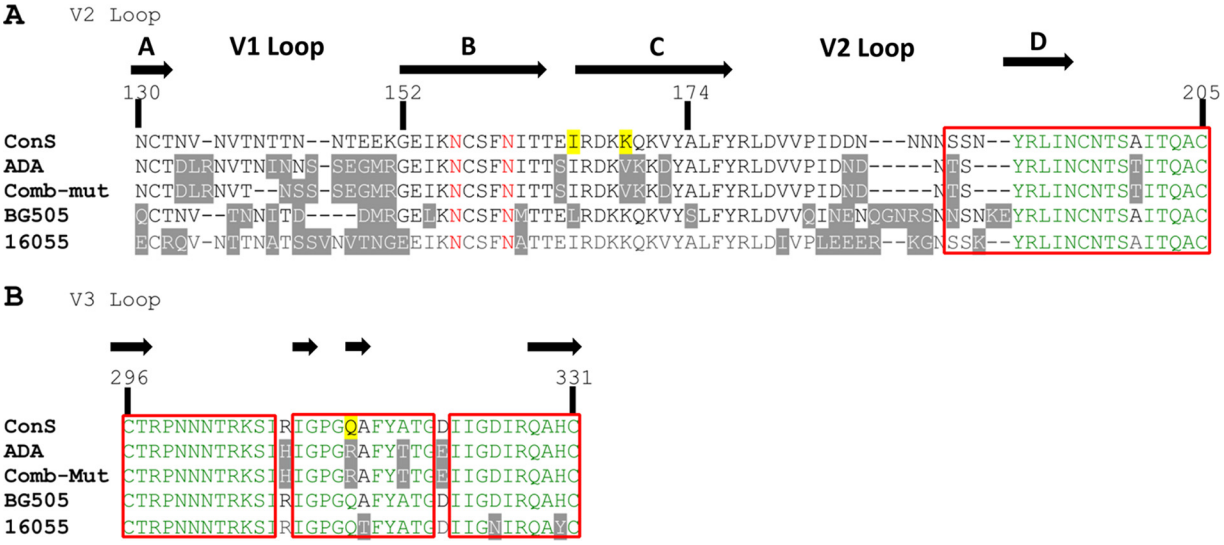

FIG 2 Alignment of V1V2 and V3 sequences. The V1V2 (A) and V3 (B) amino acid sequences of the group M consensus (ConS), ADA, Comb-mut, BG505, and 16055 were aligned using DNASTAR Lasergene ClustalW with an HxB2 numbering scheme. Highlighted in gray are residues that differ from ConS. Residues in red indicate N-linked glycosylation sites at N156 and N160. Highlighted in yellow are positions 165, 169, and 315; the former two were mutated I165L/V169K to generate ADA-LK and CM-LK, and the latter was mutated R315Q to eliminate neutralization by V3 crown antibodies. Amino acids represented in green are >50% conserved among all isolates, and those boxed in red are >50% conserved among subtype B (hiv.lanl.org). The beta-sheet structure and labeling are indicated by black arrows, based on data published by McLellan et al. for V2 (21) and Huang et al. for V3 (87).

Mutants were screened for MPN with PG9 at a concentration of 5 μg/ml, which is well into the plateau of the dose-response curve with both ADA and Comb-mut. Of the 36 mutants tested, 17 substitutions significantly enhanced neutralization of ADA by PG9, including eight outside V1V2 (Fig. 3 and Table 1). Fourteen substitutions had little effect, and another five diminished PG9 MPN (i.e., N130Q, K170Q, A174S, T200A, and I309M). Substitutions in ADA that enhanced PG9 neutralization were also introduced into Comb-mut, along with some mutations that we speculated might affect trimer stability based on analysis of the crystal structure of the stable BG505 SOSIP trimer (8). Of the substitutions that enhanced the MPN of PG9 in ADA, only I165L and V169K did so with Comb-mut; however, a trend toward a higher MPN was observed with Comb-mut S164E and D187N (Fig. 3; Table 1). Hence, only substitutions in V2, near residues 166 to 176 of the C strand, enhanced PG9 neutralization (i.e., the MPN) of both labile and stable Env trimers, i.e., ADA and Comb-mut.

Mutations I165L and V169K were combined to produce the double mutants ADA-LK and CM-LK. Combining the two substitutions enabled 100% neutralization of CM-LK by PG9 and PG16 with a reduction in IC_{50}s by 9- and 4-fold, respectively (Fig. 4 and Table 2). Neutralization curves of PG9 and PG16 increased in slope from parental virus to the double mutant (i.e., slopes of ADA and Comb-mut increased from 0.5 and 0.8 to 1.1 and 1.3 for the LK mutants, respectively). Thus, the LK mutation enhanced both potency and completeness of PG9/PG16 neutralization, suggesting that the V2 supersite became more accessible and homogeneous throughout the virion population.

Stability of ADA mutants correlates with PG9 neutralization (MPN). To determine whether substitutions that affect PG9 neutralization also affect Env stability, we turned to a stability-of-function assay we described previously that determines the temperature at which infectivity of HIV-1 decreases by 90% in 1 h involving an Env of interest pseudotyped on a constant viral backbone (i.e., a T90 assay) (45). Notably, of the 16 mutations discussed above to enhance the MPN of PG9, 6 were also significantly stabilizing for ADA (i.e., T90 increased to 45.3 to 47.3°C from 42.7°C [$P < 0.05$]), while several others trended toward stabilization (Table 1). The six mutations that stabilized ADA and enhanced PG9 MPN were in V1 (N136S and S143D), V3 (N302Y, R315Q, and A316T), and the gp41 disulfide loop region (T605P). These mutations also tended to

TABLE 1 MPN values for PG9 and functional stability (T90) of mutants of ADA and Comb-mut[a]

Strain	ADA						Comb-mut			
	PG9 MPN (%)	*t* test (PG9 MPN)	T90 (°C)	*t* test (T90)	Infectivity (% WT)	447-52D IC_{50} (μg/ml)	PG9 MPN (%)	*t* test	Infectivity (% WT)	Comment(s)
Wild type	63.6 ± 4.2		42.7 ± 0.6		100 ± 4.1	0.050	87.2 ± 3.5		100 ± 5.8	
K46A	88.6 ± 2.4	****	44.5 ± 1.3	NS	103 ± 3.0	ND	86.0 ± 3.0	NS	86 ± 2.6	Neutralization resistance in SIV (13)
E87A	81.3 ± 5.8	****	44.5 ± 1.3	NS	101 ± 8.5	ND	85.7 ± 3.3	NS	109 ± 1.4	5P12-RANTES escape (D. Mosier, unpublished)
L111A	80.2 ± 1.8	****	44.7 ± 0.5	NS	119 ± 4.7	0.13	79.1 ± 0.6	NS	16 ± 0.6	Reduced gp120 dimers (88, 89)
K121Q	ND		ND		ND	ND	86.8 ± 3.8	NS	36 ± 7.2	Structural analysis[b]
N130Q	29.2 ± 8.1	****	42.8 ± 0.8	NS	101 ± 0.5	ND	ND		ND	Sequence alignment[c]
D133N	61.0 ± 6.0	NS	42.6 ± 0.2	NS	132 ± 1.6	0.043	ND		ND	Sequence alignment
R135T	69.3 ± 3.3	NS	44.4 ± 1.4	NS	93 ± 15.0	ND	76.5 ± 3.3	**	28 ± 0.9	Sequence alignment
N136S	77.6 ± 3.6	****	47.3 ± 0.4	****	106 ± 2.5	4.7	91.6 ± 2.6	NS	89 ± 1.1	5P12-RANTES escape (D. Mosier, unpublished)
V137N	61.0 ± 8.4	NS	42.4 ± 0.2	NS	36 ± 1.6	0.022	ND		ND	Sequence alignment
S143D	79.0 ± 3.6	****	46.5 ± 1.2	***	96 ± 2.9	6.4	81.8 ± 6.8	NS	43 ± 2.6	Sequence alignment
I153L	65.6 ± 8.6	NS	42.3 ± 0.6	NS	66 ± 0.4	ND	ND		ND	Sequence alignment
I161M	59.5 ± 3.8	NS	41.8 ± 1.1	NS	48 ± 2.0	0.00064	ND		ND	Sequence alignment
S164E	77.3 ± 0.5	***	45.0 ± 0.8	NS	33 ± 1.6	0.025	89.4 ± 4.8	NS	71 ± 3.5	Sequence alignment
I165L	80.1 ± 2.7	****	43.4 ± 1.4	NS	78 ± 2.0	0.0085	94.7 ± 1.6	NS	81 ± 6.1	Sequence alignment
V169K	94.7 ± 3.2	****	43.0 ± 1.0	NS	90 ± 7.7	0.31	92.6 ± 4.2	NS	102 ± 3.9	Correlate with RV144 protection (63)
K170Q	26.0 ± 8.5	****	42.5 ± 0.5	NS	110 ± 3.8	10.3	47.2 ± 2.7	****	86 ± 0.7	Sequence alignment
D172V	59.4 ± 4.2	NS	43.7 ± 1.1	NS	59 ± 1.7	ND	69.9 ± 3.2	***	103 ± 6.1	Sequence alignment
A174S	30.2 ± 7.1	****	39.8 ± 0.4	NS	20 ± 0.8	0.00028	ND		ND	Sequence alignment
P183Q	ND		ND		ND	ND	86.7 ± 4.4	NS	67 ± 6.2	Structural analysis
N186G D187S N188S	ND		ND		ND	ND	88.8 ± 2.1	NS	70 ± 8.5	Structural analysis
D187N	80.9 ± 2.6	****	44.0 ± 0.3	NS	77 ± 2.9	0.0088	89.1 ± 4.4	NS	56 ± 4.9	Sequence alignment
T200A	52.0 ± 4.9	**	42.2 ± 0.5	NS	6 ± 0.5	ND	ND		ND	Sequence alignment
T219A	58.8 ± 6.5	NS	42.6 ± 0.6	NS	90 ± 7.5	0.33	ND		ND	Sequence alignment
N276D	72.0 ± 8.5	*	44.3 ± 0.4	NS	79 ± 4.4	31.7	87.2 ± 3.1	NS	112 ± 1.2	Knocks out N-glycosylation site
N302Y	78.0 ± 5.5	****	45.3 ± 0.7	*	66 ± 3.2	7.3	86.4 ± 2.1	NS	74 ± 3.0	5P12-RANTES escape (D. Mosier, unpublished)
I309M	37.0 ± 5.3	****	42.6 ± 0.3	NS	6 ± 0.6	0.0010	ND		ND	5P12-RANTES escape (D. Mosier, unpublished)
R315Q	77.3 ± 4.1	****	47.5 ± 0.2	**	82 ± 5.4	>100	83.0 ± 3.9	NS	114 ± 4.4	Clade C V3 consensus (90)
A316T	73.6 ± 1.9	**	46.2 ± 1.7	***	91 ± 4.5	55.5	83.2 ± 3.1	NS	108 ± 3.9	Clade C V3 consensus (90)
A316W	ND		ND		ND	ND	85.8 ± 2.9	NS	39 ± 2.4	Structural analysis
F317W	66.2 ± 6.0	NS	41.2 ± 0.5	*	12 ± 1.0	0.0034	ND		ND	5P12-RANTES escape (D. Mosier, unpublished)
Y318F	63.5 ± 3.0	NS	42.8 ± 0.9	NS	114 ± 6.1	0.036	ND		ND	5P12-RANTES escape (D. Mosier, unpublished)
T319A	66.2 ± 4.5	NS	46.2 ± 0.4	**	116 ± 4.7	43.0	83.7 ± 1.3	NS	23 ± 1.7	Clade C V3 consensus (90)
T320W	ND		ND		ND	ND	87.7 ± 3.2	NS	130 ± 3.8	Structural analysis
I420M	ND		ND		ND	ND	86.4 ± 3.1	NS	68 ± 3.9	Structural analysis
R440A	85.9 ± 0.6	****	44.8 ± 1.4	NS	102 ± 2.1	21.3	80.3 ± 3.8	NS	105 ± 5.1	Structural analysis
R440Q	ND		ND		ND	ND	86.8 ± 5.2	NS	87 ± 2.5	Structural analysis
Q442V	ND		ND		ND	ND	88.0 ± 4.5	NS	86 ± 2.3	Structural analysis
N461G	69.3 ± 3.8	NS	44.0 ± 0.5	NS	126 ± 16.1	1.3	82.4 ± 2.3	NS	97 ± 6.9	Knocks out N-glycosylation site
N553S	79.5 ± 4.2	****	44.4 ± 1.5	NS	95 ± 5.7	0.59	83.4 ± 2.4	NS	97 ± 3.4	Stabilized gp140 trimer (91)
I559Y	64.6 ± 2.9	NS	44.9 ± 0.6	NS	19 ± 2.3	ND	67.7 ± 2.9	****	11 ± 0.6	Structural analysis
L565M	61.0 ± 3.3	NS	46.0 ± 0.4	**	104 ± 8.7	1.2	ND		0 ± 0.0	5P12-RANTES escape (D. Mosier, unpublished)
Q567K	71.4 ± 2.4	*	46.3 ± 0.3	**	76 ± 4.7	64.7	84.0 ± 2.0	NS	82 ± 4.2	Stabilized gp140 trimer (91)
T605P	78.4 ± 3.9	****	47.7 ± 1.2	****	103 ± 3.7	12.6	85.8 ± 2.3	NS	70 ± 5.0	Identified from drug screen (DPL)
A612S	64.6 ± 4.2	NS	44.7 ± 0.2	NS	95 ± 2.9	1.76	84.5 ± 3.8	NS	88 ± 1.6	Identified from drug screen (DPL)

[a]PG9 maximum percent neutralization (MPN) was determined at 5 μg/ml. ND, not determined; NS, not significant. *, $P \leq 0.05$; **, $P \leq 0.01$; ***, $P \leq 0.001$; ****, $P \leq 0.0001$. The "Infectivity (% WT)" columns indicate the percentages of wild-type virus infectivity ± the standard deviation.

[b]These mutations in subunit interfaces were anticipated to impact Env trimer stability and conformation based on analysis of an X-ray crystal structure of BG505 SOSIP gp140 (8).

[c]After sequence alignments, the amino acid residues in ADA/Comb-mut were changed to that of HIV-1 isolates BG505 or 16055, which are fully neutralized by PG9 and PG16.

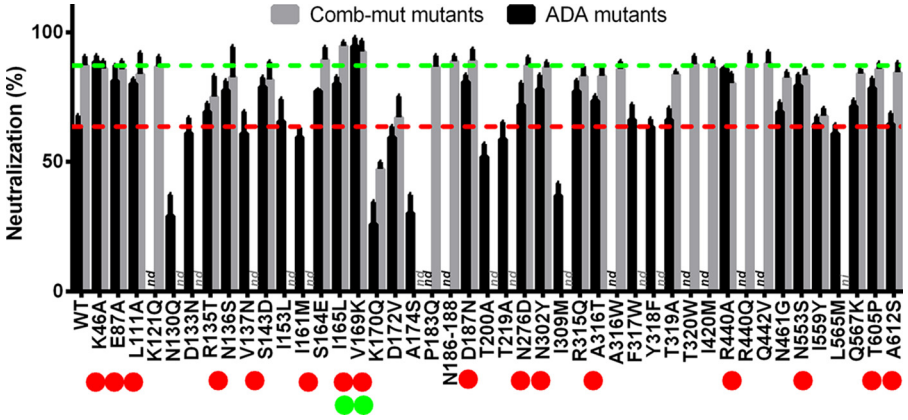

FIG 3 Neutralization (MPN) of mutant Envs of HIV-1 ADA and Comb-mut by PG9. Substitutions were introduced into ADA pseudovirus and mutants were tested for sensitivity to PG9 neutralization at a constant concentration of 5 μg/ml. A subset of substitutions that showed a significant increase in MPN was then similarly tested in a Comb-mut Env background. Certain mutations that were predicted by structural analysis to potentially affect V2 and V3 antibody neutralization were also tested in Comb-mut but not ADA. Mutations that were not tested in a given background are labeled "nd" (not determined) or "ni" (not infectious). "N186-188" represents the triple mutant N186G/D187S/N188S. The red and green dashed lines indicate MPNs for wild-type ADA and Comb-mut, respectively. Red dots indicate mutants that show enhanced PG9 neutralization relative to wild-type ADA, green dots indicate enhanced PG9 neutralization of both ADA and Comb-mut. Each bar represents an average of biological triplicate values.

show higher MPN values of PG9 against ADA (Table 1). Notably, when all mutations were analyzed, a statistically significant positive correlation ($P = 0.0004$) was observed between T90 and MPN of PG9 (Fig. 5A). No correlation was observed between T90 and PG9 IC_{50} ($P = 0.3244$; data not shown). Altogether, a total of 14 mutations stabilized ADA while showing positive effects on PG9 neutralization.

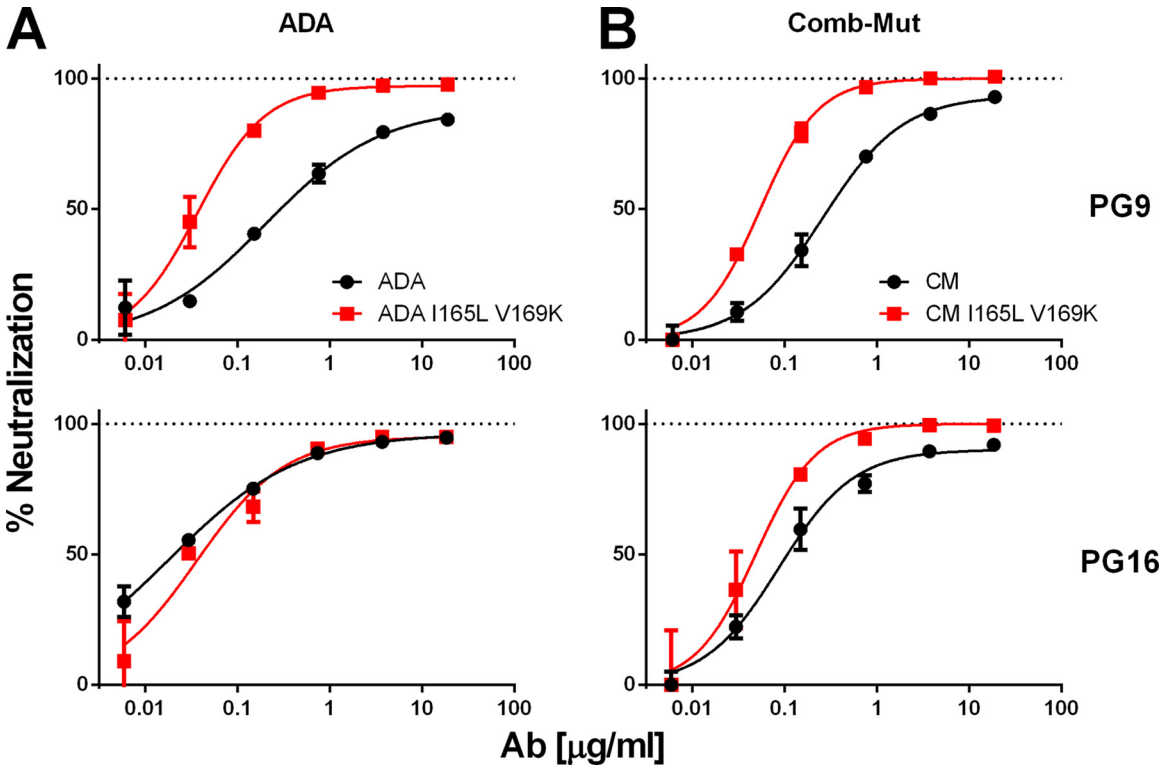

FIG 4 Comb-mut containing V2 substitutions I165L and V169K is neutralized completely and efficiently by PG9 and PG16. ADA (A) and Comb-mut (B) parental pseudoviruses (black circles), as well as I165L V169K double mutants (red squares), were assayed for neutralization against PG9 (top panels) and PG16 (bottom panels). Experiments were performed in triplicate.

TABLE 2 Substitutions I165L and V169K enhance neutralization of HIV-1 ADA and Comb-mut by PG9 and PG16

	PG9			PG16		
Virus	IC_{50} (μg/ml)	MPN (%)	Slope	IC_{50} (μg/ml)	MPN (%)	Slope
ADA WT	0.272	88	0.59	0.026	94	0.56
ADA I165L	0.067	96	0.59	0.010	98	0.63
ADA V169K	0.016	99	0.49	0.006	99	0.49
ADA-LK	0.034	97	1.10	0.037	96	0.79
Comb-mut WT	0.268	92	0.89	0.099	92	0.80
Comb-mut I165L	0.158	99	0.79	0.048	98	1.26
Comb-mut V169K	0.037	100	0.83	0.017	98	1.98
CM-LK	0.030	100	1.38	0.022	100	1.33

The functional stability (T90) of Comb-mut was determined to be at the maximum limit possible with the infectivity-based assay (i.e., T90 ~50°C), since components of the viral backbone inactivate around this temperature (44, 45). All of the Comb-mut mutants were similarly at the maximum T90 value for this assay and so are most likely

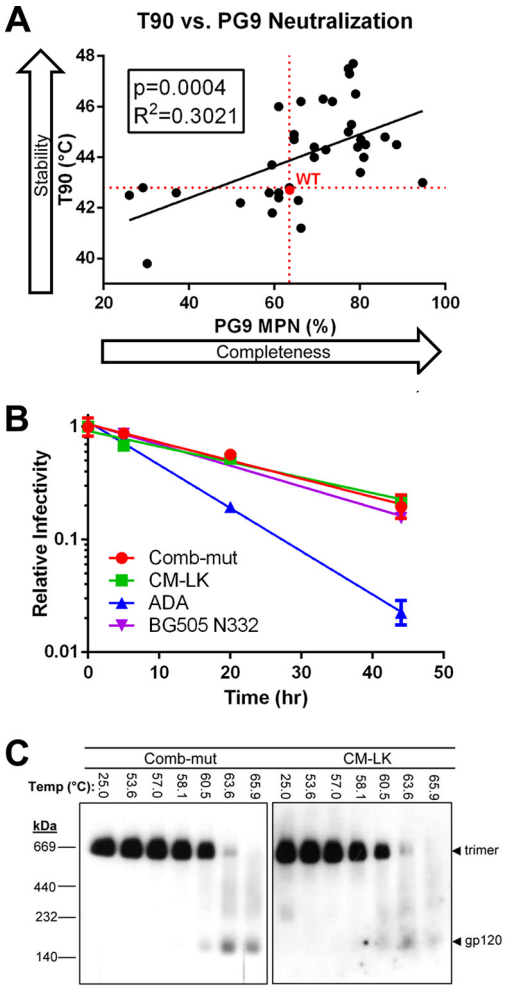

FIG 5 Stability of Env correlates with enhanced MPN of PG9 and decreased neutralization by 447-52D. (A) Mutants of ADA were tested for thermostability and neutralization by PG9. T90 values are plotted against the percent neutralization at 5 μg/ml of PG9. A statistically significant relationship was observed between increased Env stability and an increase in PG9 neutralization. (B) Infectivity decay at 37°C of ADA, Comb-mut, and CM-LK. The results of a representative experiment performed in triplicate are shown, and the error bars represent the standard deviations. (C) Physical thermostability of Comb-mut and CM-LK Env trimers. BN-PAGE Western blot analysis of trimeric Envs solubilized from heat-treated virus shows that I165L/V169K do not change the trimer stability of Comb-mut.

comparable in stability to Comb-mut. Because I165L and V169K improved PG9/PG16 neutralization of ADA and Comb-mut without affecting the T90, we further tested Comb-mut and its mutant CM-LK for infectivity decay at 37°C, as well as its physical trimer stability. (We note that Comb-mut trimers previously showed higher physical stability than ADA in a temperature gradient Blue Native-PAGE [BN-PAGE] assay by ~12°C [44].) No differences between Comb-mut and CM-LK were observed in the half-life of infectivity decay at 37°C or in the integrity of heat-treated Env trimers on BN-PAGE (Fig. 5B and C). We conclude that I165L and V169K enhance PG9/PG16 neutralization without altering Env trimer stability and hence are distinct from the many non-V2 mutations in which Env ADA stability and MPN of PG9 appear to be linked.

Mutations I165L and V169K enhance neutralization of ADA by several V2 bnAbs. We assayed ADA-LK and CM-LK for neutralization by additional V2 bnAbs including, PGT145 (15), CH01 (22), VRC26.08 (16), and PGDM1400 (17). As with PG9 and PG16, PGDM1400 neutralized ADA-LK and CM-LK with IC_{50}s lower than parental viruses and with 100% neutralization, which is consistent with the superior breadth of PGDM1400 (Fig. 6A) (17). ADA and Comb-mut were resistant to VRC26.08 and CH01, but the LK substitution made these viruses highly sensitive to VRC26.08 and partially sensitive to CH01 (MPN of ~40%), which lends support to the reported dependence of these bnAbs on K169 (48).

PGT145 was an exception, however, since the LK mutation caused IC_{50}s to increase 5- to 10-fold and MPNs to decrease from 100% to 82 to 91% (Fig. 6A). The effect was localized because ADA-LK and CM-LK showed no change in sensitivity to non-V2 bnAbs, including those against the CD4bs, N332 glycan, and MPER of gp41 (Fig. 6A; data not shown). Further analysis showed that V169K was largely responsible for the observed changes in PGT145 and VRC26.08 neutralization (Fig. 6B).

We also compared the neutralization sensitivity of ADA, ADA-LK, Comb-mut, and CM-LK toward gp120-gp41 interface bnAbs PGT151, 35O22, and 3BC176, since these bnAbs are known to only partially neutralize many isolates (49–51). Interestingly, Comb-mut was much more completely and potently neutralized by all three Abs than ADA (Fig. 6C). This effect could be the result of a shift in a gp41 glycan at the gp120-gp41 interface from N624 in ADA to N625 in Comb-mut (44). 35O22 depends on the glycan at N625 and, whereas an N625 glycan-knockout does not strongly affect neutralization by either PGT151 or 3BC176, the 624/625 glycan shift may perhaps alter their epitopes given the extreme proximity of these residue positions (49–51). The LK mutations did not significantly improve the MPN of the interface bnAbs against Comb-mut, but Comb-mut is already neutralized 100% by PGT151 and 96% by 35O22. However, PGT151 neutralization of ADA was improved by these mutations (ADA = 23% MPN; ADA-LK = 55% MPN), which suggests that these mutations generally increase the homogeneity of Env even at distal sites.

We further tested the sensitivity of ADA, ADA-LK, Comb-mut, and CM-LK to soluble CD4 (sCD4) as another measure of the effect of I165L and V169K on Env stability, since resistance to sCD4 has been associated with greater Env stability (44, 52). As previously reported (44), Comb-mut was more resistant to sCD4 than ADA by ~70-fold (Fig. 6C). The LK mutations had little effect on sCD4 inhibition of Comb-mut, supporting the BN-PAGE data showing that Comb-mut and CM-LK are roughly equal in stability (Fig. 5C). I165L and V169K increased sensitivity of ADA to sCD4 by ~5-fold, which is a somewhat specific effect since thermostability was unaffected by these two mutations in ADA (Table 1).

Blocking complex glycosylation alters V2 bnAb neutralization of ADA/Comb-mut mutants. Blocking the trimming of high-mannose on N-linked glycosylation of HIV-1 Env affects neutralization by V2 bnAbs (4). We investigated this aspect of glycan processing on neutralization of ADA/Comb-mut and cognate LK mutants. Pseudotyped viruses were produced under different conditions to generate trimmed N-linked glycans: (i) in $GnTI^{-/-}$ (293S) cells that produce Man5-9GlcNAc2 (4), (ii) in 293T cells treated with kifunensine that generate Man9GlcNAc2 (53), or (iii) in cells treated with

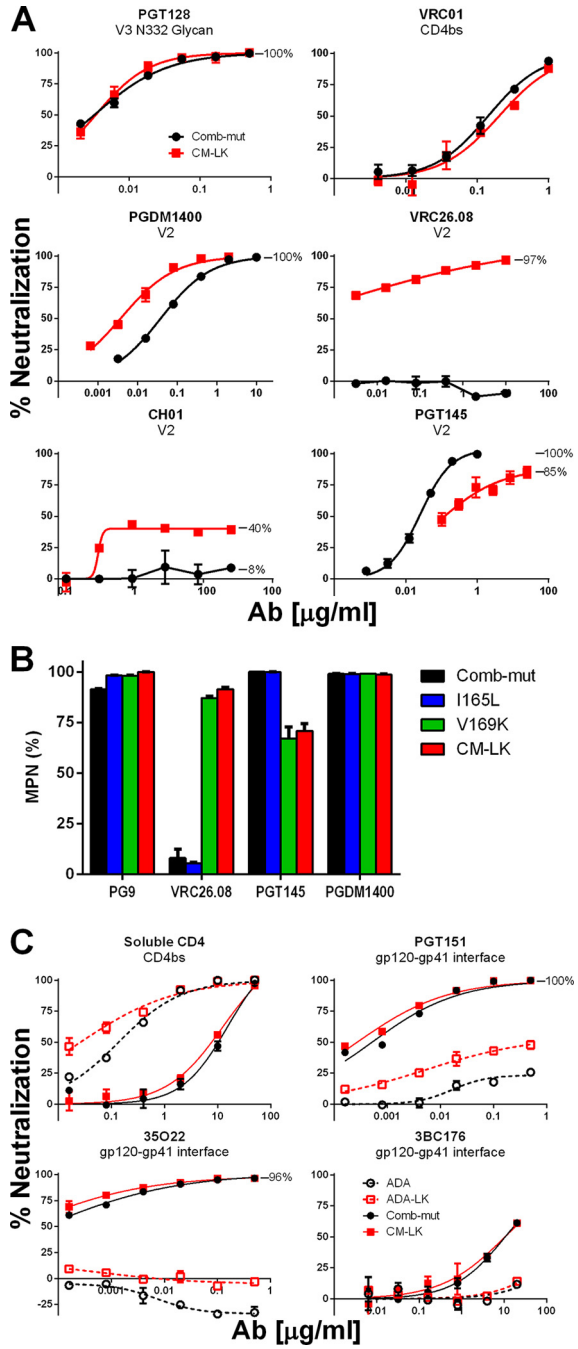

FIG 6 Neutralization of Comb-mut and CM-LK by V2 antibodies. (A) Comb-mut and CM-LK pseudotyped viruses were tested against various V2 bnAbs, as well as control antibodies PGT128 and VRC01. (B) The MPN of V2 bnAbs is shown against Comb-mut, CM-LK, and the constituent mutations of CM-LK, I165L and V169K. (C) ADA, ADA-LK, Comb-mut, and CM-LK pseudotyped viruses were tested in TZM-bl neutralization assays against gp120-gp41 interface bnAbs and the soluble form of the HIV-1 receptor, CD4. Data shown are from a representative experiment performed in triplicate, and error bars represent the standard deviations from the mean.

swainsonine that results in GlcNAcMan5GlcNAc2 with possible hybrid glycans on the third arm (4). Kifunensine-treated viruses were resistant to all of the V2 bnAbs tested, a finding consistent with prior studies (data not shown) (4, 17). However, production of Env in the presence of swainsonine or in 293S cells had various effects on different Ab-Env combinations. First, swainsonine reduced the MPN of PGT145 against the LK mutants and not wild-type viruses; 293S cell production did not have this effect (Fig. 7A

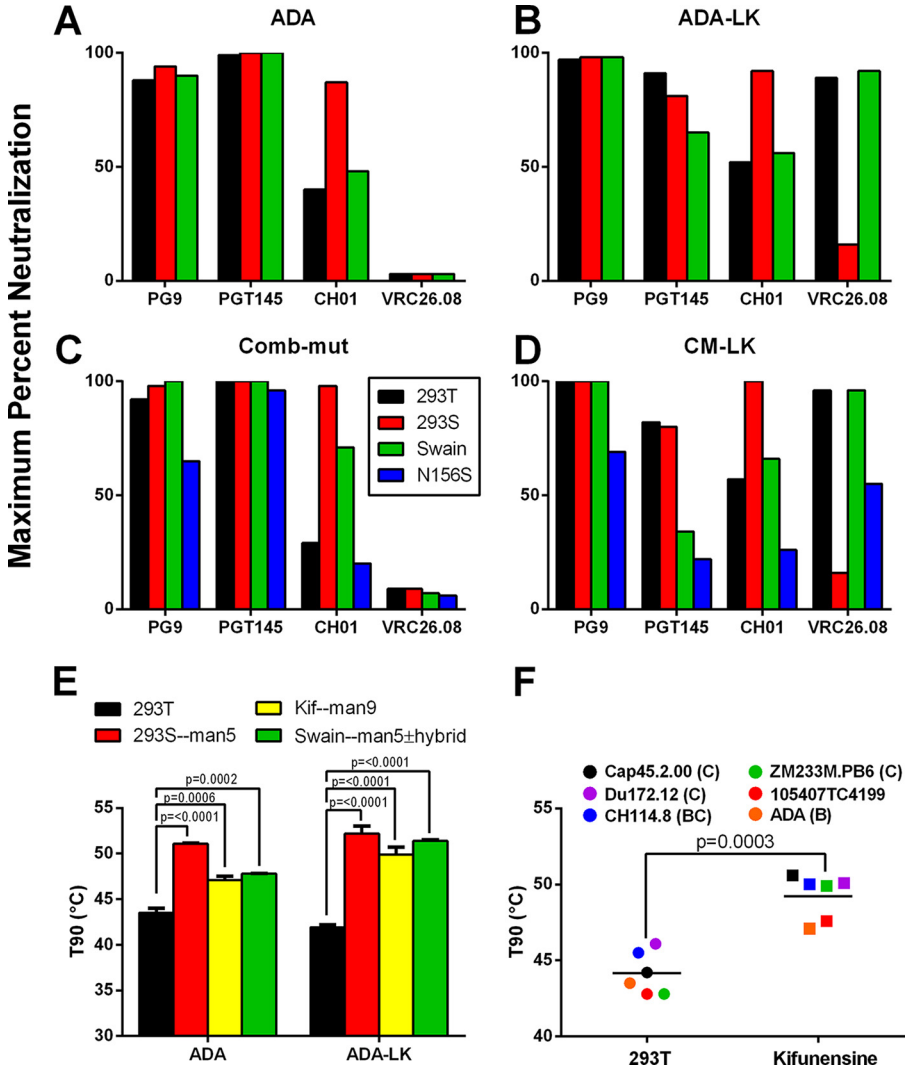

FIG 7 Neutralization properties of glycosylation-modified HIV-1 ADA, ADA-LK, Comb-mut, and CM-LK Env by V2 bnAbs. ADA (A), ADA-LK (B), Comb-mut (C), and CM-LK (D) pseudotyped viruses were generated in 293T cells, in 293S cells, or in the presence of swainsonine. Virions of Comb-mut and CM-LK that had the N156S mutation, which eliminates the glycosylation site at this position, were also generated in 293T cells. Viruses were tested in neutralization assays against V2 bnAbs PG9, PGT145, CH01, and VRC26.08. The MPN findings are shown in panels A to D. (E) The stability of ADA wild-type and ADA-LK virion Envs produced in 293T or 293S cells or in the presence of kifunensine or swainsonine was tested in a T90 assay. A statistically significant increase in the functional stability of Env was found with each treatment relative to producing virus in 293T cells. The statistical significance was determined using a paired two-tailed *t* test. (F) Six different viruses from different clades were produced with or without the addition of kifunensine, and the functional stability was tested in the T90 assay.

to D; Table 3). Second, producing virus in 293S cells increased the MPN of CH01 in all cases, reaching 100% against CM-LK. Third, VRC26.08 neutralization was abrogated when virus was produced in 293S cells. Lastly, swainsonine treatment increased sensitivity of ADA-LK and CM-LK to VRC26.08 without increasing MPNs. The latter three findings suggest that CH01 binds better to terminal mannose glycans, whereas VRC26.08 prefers complex glycosylation.

The glycan contacts with V2 bnAbs in structural models mainly involve N160, with N156 supplying secondary contacts (21, 28–30, 54). We made knockouts of these glycans in Comb-mut and CM-LK and assayed virus sensitivity to the V2 bnAbs used above. As expected, N160A abolished neutralization by all antibodies (data not shown). N156S had little effect on PGT145 neutralization of Comb-mut and diminished the PG9 IC_{50} 5-fold (Fig. 7C and D; Table 3). In contrast, N156S in the CM-LK background reduced

TABLE 3 Neutralization of glycosylation-modified pseudotyped virus by V2 bnAbs

	293T		293S		Swainsonine		N156		N160	
nAb	IC_{50} (μg/ml)	MPN (%)	IC_{50} (μg/ml)	MPN (%)	IC_{50} (μg/ml)	MPN (%)	IC_{50} (μg/ml)	MPN (%)	IC_{50} (μg/ml)	MPN (%)
ADA										
PG9	0.27	88	0.35	94	0.12	90	ND[a]	ND	ND	ND
PGT145	0.10	99	0.08	100	0.02	100	ND	ND	ND	ND
CH01	>25	40	0.83	87	>25	48	ND	ND	ND	ND
VRC26.08	>25	3	>25	22	>25	3	ND	ND	ND	ND
ADA-LK										
PG9	0.03	97	0.78	98	0.40	98	ND	ND	ND	ND
PGT145	0.39	91	1.31	81	8.02	65	ND	ND	ND	ND
CH01	20.10	52	1.82	92	13.40	56	ND	ND	ND	ND
VRC26.08	0.52	89	>25	16	0.05	92	ND	ND	ND	ND
Comb-mut										
PG9	0.27	92	0.23	98	0.08	100	1.39	65	>25	16
PGT145	0.08	100	0.07	100	0.05	100	0.02	96	>25	15
CH01	>25	29	0.45	98	2.77	71	>25	20	>25	19
VRC26.08	>25	9	>25	29	>25	7	>25	6	>25	16
CM-LK										
PG9	0.03	100	0.19	100	0.38	100	2.40	69	>25	0
PGT145	1.00	82	0.76	80	>25	34	>25	22	>25	0
CH01	7.58	57	0.34	100	7.99	66	>25	26	>25	0
VRC26.08	0.17	96	>25	16	0.03	96	>25	55	>25	36

[a]ND, not determined.

the PG9 IC50 80-fold, abrogated neutralization by PGT145, and severely reduced neutralization by both CH01 and VRC26.08. We assume that the glycan knockout at N156 alters glycosylation at N160 or its packing with the B and C strands as a part of the V2 epitope (54), thereby increasing the dependence of all of the V2 bnAbs on the glycan at N156.

Preventing complex glycosylation increases thermostability of Env. We wished to determine whether blocking complex glycosylation affected the functional stability of Env. Thus, ADA and ADA-LK glycosylation modified variants were assessed for thermostability using the heat gradient (T90) assay. Kif-, swain-, and $GnTI^{-/-}$ cell-treated viruses all showed enhanced T90s that went from ~42°C to 47 to 51°C (Fig. 7E). Hence, blocking complex glycosylation and/or mannose trimming generally increased the thermostability of ADA. The Comb-mut variants showed maximum T90 values irrespective of the glycosylation modifications, suggesting that the stable Comb-mut trimer is at least not destabilized by changes in glycosylation. To determine whether blocking complex glycosylation and mannose trimming is stabilizing for other Envs, a panel of pseudotyped viruses of modest stability (i.e., T90s ~43 to 46°C) was similarly produced in the presence or absence of kifunensine and tested for thermostability. Five of five viruses showed increased T90s when produced in the presence of kifunensine ($P = 0.0003$). Taken together, our data show that complex glycosylation is generally unfavorable for functional stability, at least with moderately stable Envs.

PG9 and PGT145 together fully neutralize mixed Env trimers. Incomplete neutralization by a V2 bnAb might arise from variation in glycosylation or folding that occludes the three potential binding sites on the trimer. However, it is unclear whether or how adjacent protomers influence this resistance. We performed a mixed trimer experiment in which Env plasmids of Comb-mut and CM-LK—which show partial resistance to PG9 and PGT145, respectively—were mixed 1:1 prior to preparing pseudotyped virus. Neutralization assays were performed using PG9, PGT145, and a cocktail of the two bnAbs. We found that mixed-trimer virus was partially resistant to single bnAbs and fully neutralized by the double bnAb cocktail (Table 4). These results support a model in which mixing protomers does not cause resistance to both bnAbs that would have indicated supraheterogeneity in mixed subunit interfaces.

TABLE 4 HIV-1 with mixed Comb-mut/CM-LK Env trimers is neutralized completely by combining PG9 and PGT145

	PG9		PGT145		PG9+PGT145	
Virus	IC_{50} (μg/ml)	MPN (%)	IC_{50} (μg/ml)	MPN (%)	IC_{50} (μg/ml)	MPN (%)
Comb-mut	0.27	92	0.08	100	0.01	100
CM-LK	0.03	100	1.00	82	0.03	100
Comb-mut/CM-LK	0.09	98	0.06	97	0.07	100

V2 bnAbs with higher MPNs bind to a greater proportion of Env trimers. Incomplete neutralization of virus by V2 bnAbs presumably results from a failure to recognize a subpopulation of Env. To investigate, we coincubated V2 bnAbs with Comb-mut and CM-LK virions, detergent solubilized the Env-bnAb complexes, and visualized the complexes using a gel mobility shift assay employing BN-PAGE and Western blotting. Several observations were notable. First, PG9 and PG16 completely shifted the band corresponding to CM-LK trimers, but with Comb-mut a fraction of trimers remained unshifted, which suggests that I165L/V169K overcomes microheterogeneity in Comb-mut to allow binding to all of its spikes (Fig. 8A). Second and surprisingly, PGT145 and PGDM1400 did not fully shift the Comb-mut trimer band despite achieving 100% MPNs and totally failed to shift CM-LK spikes. Gel mobility shifts were also absent with VRC26.08 and CH01 against both viruses, even though they partially neutralized CM-LK.

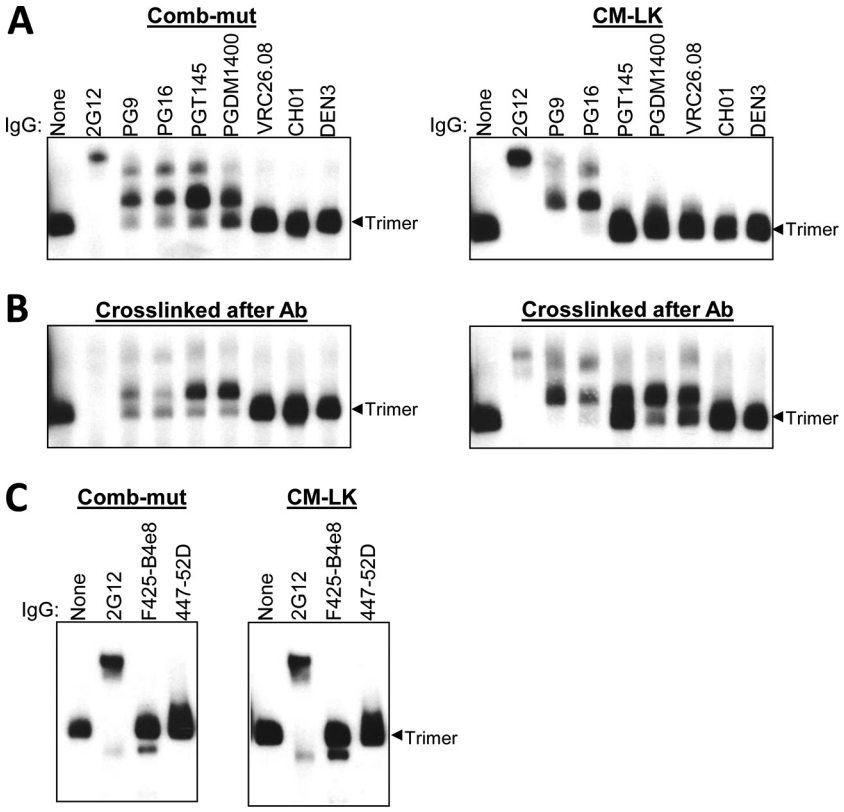

FIG 8 BN-PAGE gel mobility shift of Comb-mut and CM-LK trimeric Env in the presence of various bnAbs. (A) Comb-mut and CM-LK virions, displaying >95% cleaved Env, were incubated in the presence of the IgGs specified (25 μg/ml) and analyzed using BN-PAGE Western blot. Binding of an antibody causes the Env trimer to run more slowly on the gel, thus shifting the band upward on the blot. 2G12 and DEN3 were used as positive- and negative-control antibodies, respectively. (B) Virion-antibody complexes were fixed using the chemical cross-linker BS^3—after antibody binding but before adding detergent—to prevent antibodies from falling off during the gel run. (C) Comb-mut and CM-LK virions were incubated with 447-52D or F425-B4e8 IgGs that bind to V3, or control IgG 2G12, and then Env trimers were solubilized using detergent and analyzed using a BN-PAGE Western blot.

We suspected that, where there was a lack of correlation between gel mobility shift and neutralization, bnAbs might have dissociated from Env, either following detergent treatment or during electrophoresis. To test this hypothesis, we cross-linked bnAb-virion complexes prior to adding detergent (37). Cross-linking increased the apparent occupancy of V2 bnAbs on Env spikes in almost all cases in which V2 bnAbs neutralized and gel shifts were inefficient (Fig. 8B). This is most prominently seen with PGDM1400 and VRC26.08 against CM-LK, perhaps because these antibodies are particularly sensitive to the quaternary state of Env and therefore might dissociate from the spikes most easily upon detergent treatment (16, 17). CH01 failed to produce a shift; however, CH01 only neutralizes CM-LK with an MPN of ~40%, so occupancy appears to be transient and limited with this antibody. Taken together, the BN-PAGE data broadly align with the neutralization results and imply that substitution LK alters the antibody-binding site to make the virus/Env population uniformly recognizable to PG9, PG16, and VRC26.08, but not to PGT145.

V3 crown neutralization correlates inversely with stability of ADA. The spike of Comb-mut is more physically thermostable than a variety of tier 1 and tier 2 primary isolates (44, 45). Comb-mut was modestly sensitive to V3 crown antibodies 447-52D and F425-B4e8 (Fig. 1B; IC_{50}s ~10 μg/ml), which was surprising since Comb-mut is resistant to other V3 crown antibodies, CD4bs antibodies b6 and F105, and CD4i antibodies 17b and X5. We screened various ADA mutants against 447-52D and found a significant inverse correlation between the T90 and the IC_{50} values of 447-52D ($P = <0.0001$; Fig. 9A). There was also a positive relationship between decreased 447-52D potency and the increased MPN of PG9, and this relationship attained statistical significance if V2 mutations in the PG9 interface were excluded (Fig. 9B). Taken together, we conclude that Env trimer stabilization tends to reduce exposure of V3 at the apex of the spike.

Antibodies to the V3 crown can neutralize HIV either by binding to Env prior to attachment with CD4 or postattachment (55). We tested the ability of 447-52D and F425-B4e8 to bind to unliganded trimers on Comb-mut and CM-LK virions using a BN-PAGE gel mobility shift assay (44, 56). F425-B4e8 showed no binding or shifting of the Env trimer on BN-PAGE (Fig. 8C). 447-52D did cause the trimer to "trail" upwards slightly on the gel; however, this was not a clean shift of the trimer as with control antibody 2G12. We infer from these results that 447-52D interacts only very weakly or transiently with Comb-mut and CM-LK unliganded trimers, if at all, and neutralizes these viruses when Env is in another conformation (e.g., post-CD4 engagement).

Mutation of Env to further attenuate V3 crown recognition. Given the possible relevance of V3 crown exposure to vaccine design, we assessed the neutralization sensitivity of CM-LK—the mutant most fully neutralized by the majority of V2 bnAbs—using V3 crown antibodies 447-52D and F425-B4e8. Similar to Comb-mut, it was modestly sensitive to these antibodies (Fig. 9C). 19b and 39F and coreceptor-binding site antibody 17b showed no capacity to neutralize CM-LK (data not shown). We screened 22 mutants of Comb-mut for neutralization by V3 crown antibodies and V2 bnAbs. Of the mutations we tested, only R315Q, which converts the V3 crown from the consensus motif of clade B to that of clades A and C (i.e., GPGR→GPGQ) abrogated neutralization by both 447-52D and F425-B4e8 (Fig. 9C; data not shown) (57). Notably, R315Q also increased the MPN of PG9 against ADA and stabilized ADA with a T90 increasing from 42.7 to 45.6°C (Fig. 3; Table 1). Although the mechanism of trimer stabilization by R315Q is not obvious, in the crystal structure of BG505 SOSIP, position 315 is buried in the trimer interface so changing R to Q might tend to reduce V3 crown solvent exposure and/or instability possibly involving proximal residues near to the C strand, such as N197 or K121 (Fig. 10) (54, 58). Importantly, R315Q did not alter neutralization properties of CM-LK relating to other bnAbs, except for a slight reduction in MPN of CH01 (Fig. 9C; data not shown). Thus, the triple mutant, CM-LKQ, retained the relative trimer stability of Comb-mut with added accessibility to V2 bnAbs and disruption of V3 crown epitopes at the apex of the trimer.

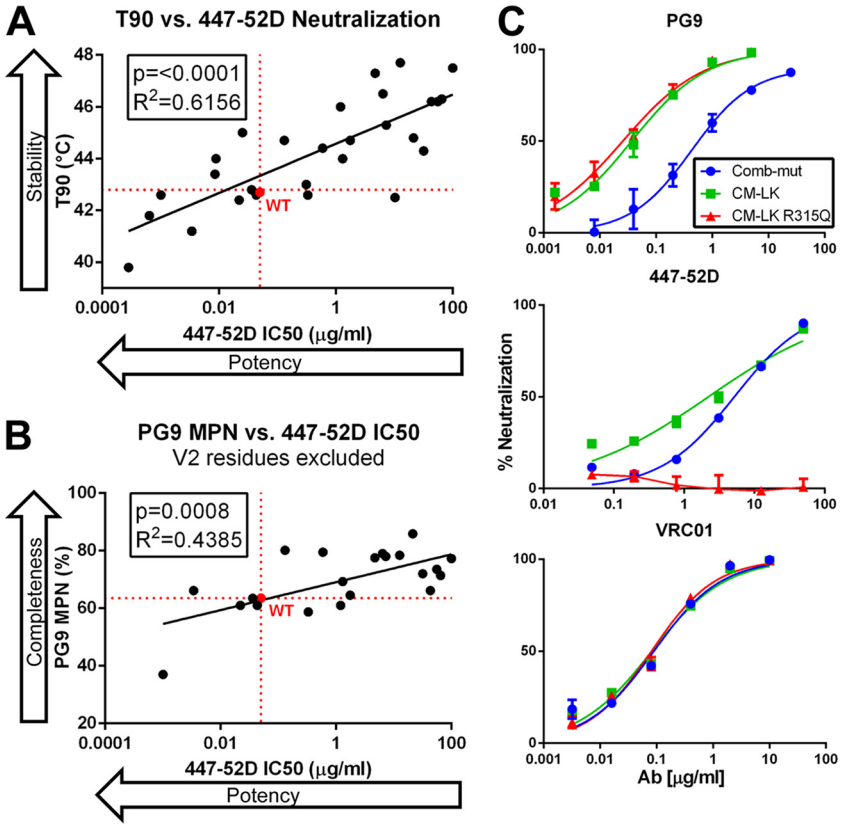

FIG 9 V3 crown neutralization correlates inversely with trimer thermostability and PG9 neutralization (MPN). (A) T90 values of mutants of ADA are plotted against the IC_{50} of V3 antibody 447-52D. A statistically significant relationship is seen between increased Env stability and a decrease in 447-52D neutralization. (B) The IC_{50} of 447-52D is plotted against the MPN at 5 μg/ml of PG9. Mutants in the V2 domain (between amino acids 160 and 190) that might directly affect PG9 binding were removed from the analysis. (C) Neutralization of Comb-mut, CM-LK, and CM-LK R315Q pseudovirions by a panel of antibodies shows that R315Q abrogates neutralization by V3 crown antibody 447-52D (middle panel) without altering the neutralization properties of PG9 (top panel) and VRC01 (bottom panel). Data shown are from a representative experiment performed in triplicate, and error bars represent the standard deviations from the mean.

DISCUSSION

HIV-1 Env trimer stability and heterogeneity can contribute to viral fitness, the former by ensuring prolonged infectivity and the latter by facilitating the evasion of host antibodies. However, these properties of Env are also significant variables in vaccine design. Incomplete neutralization or shallow dose-response curves observed with V2, V3, and CD4bs antibodies against the labile ADA isolate revealed heterogeneity in Env. We studied the relationship between Env functional stability and neutralization by V2 and V3 antibodies among mutants of ADA and hyperstable Comb-mut Env backgrounds. We found a positive correlation between Env stability and MPN of V2 bnAb PG9, as well as an inverse correlation between stability and sensitivity to V3 crown antibodies. In the process, we identified changes in Env that enhance neutralization by V2 bnAbs, stabilize native trimers, and abrogate neutralization by V3 crown antibodies. A relatively stable, homogeneous Env trimer is described that combines these features (e.g., Comb-mut LKQ).

We identified 17 mutations (out of 36) throughout ADA within and outside V2 and V3 that enhanced PG9 neutralization, 9 of which stabilized Env, and 17 that reduced V3 crown neutralization (Fig. 10). These stabilizing mutations (i.e., N136S, S143D, N302Y, R315Q, A316T, F317W, T319A, L565M, Q567K, and T605P) might be useful in engineering other Env trimer immunogens considering that these positions are relatively conserved. Some of the stabilizing mutations, e.g., N136S (V1), N302Y (V3), and L565M

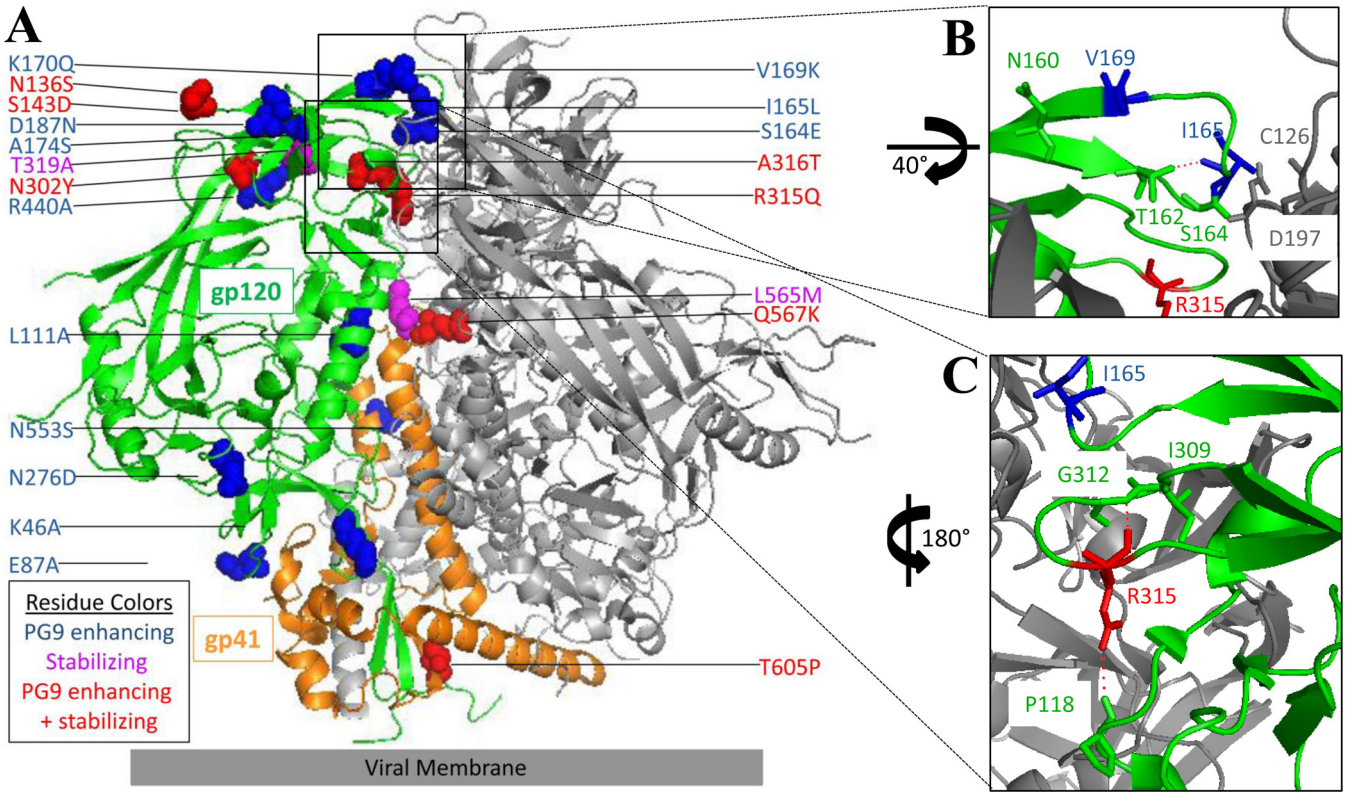

FIG 10 Location on Env of mutations that increase trimer stability or V2 neutralization. (A) Mutations that were found to increase PG9 neutralization or increase trimer stability are indicated as spheres on the crystal structure of JRFL envelope (PDB 5FYK). In the inset images, key residues at positions 165 and 169 (B) and position 315 (C) of gp120 are shown with residues nearby that may interact with them. Hydrogen bonds between neighboring amino acid residues, predicted using PyMOL, are shown using red dashed lines. I165 and R315 are shown in both inset images for orientation.

(HR1), had arisen during escape from the CCR5 inhibitor, 5P12-RANTES (47), whereas others, e.g., T605P (DSL) and A612S (HR2), had facilitated escape from the fusion inhibitor PF-68742 (D. P. Leaman and M. B. Zwick, unpublished observations). Notably, others have also reported on fusion inhibitor-escape mutations that were trimer stabilizing (59, 60). Perhaps mutations that escape fusion inhibition are often trimer stabilizing because they act to tighten subunit interfaces in order to restrict inhibitor binding.

Recently, Herschhorn et al. identified a number of mutations in V1V2 that increased sensitivity of HIV-1 to CD4 mimics, V3 MAbs, CD4i MAbs, weakly neutralizing CD4bs MAbs, and cold inactivation, but decreased sensitivity to small-molecule inhibitors of CD4-induced conformational changes, as well as to V2 and CD4bs bnAbs (52). Single-molecule FRET analysis showed that these mutations caused Env to adopt a less stable, more open conformation that the authors described as a local energy well (state 2) in between unliganded Env (state 1) and fully CD4-bound Env (state 3). Beauparlant et al. identified mutants of Env, including I165K and F317L, which showed increased infectivity toward CD4-deficient target cells and were also hyper-sensitive to CCR5 inhibitors, V3, CD4i, and weak CD4bs Abs; these authors surmised that it was in a conformation similar to the state 2 described by Herschhorn et al. (61). Most likely, the mutations that we found which stabilized Env and decreased exposure of V3 are stabilizing state 1, while mutations that did the opposite are destabilizing state 1, while favoring the adoption of state 2. However, the activation barrier between states 1 and 2 might also be affected, so to parse out the energetic states involved more detailed studies would be needed.

How does increasing trimer stability reduce IC_{50}s and improve the MPN of nAbs to the V3 crown and V2 (N160), respectively? Mutations that increase trimer stability might

raise IC_{50}s of V3 crown Abs by limiting the conformations and/or duration of V3 crown exposure before it "reburies" in the trimer, thus lowering the on rate and narrowing the range of antibody affinities for the spike. We observed a correlation between Env stability and the MPN (but not the IC_{50}) of PG9. V2 bnAbs, including PG9, may recognize a more stable conformation of the trimer than the V3 crown antibodies, so changes in trimer stability may have less of an effect on the IC_{50}s of V2 bnAbs. Mutations that improve the MPNs of V2 bnAbs might relate to improved recognition of Env as it becomes more uniformly glycosylated and folded, either in the unliganded state, the asymmetric bnAb-bound state, or both of these states.

We found that neutralization by V2 bnAbs improved due to mutations I165L and V169K. L165 is a contact residue in a complex between V2 peptide and PG9 (21) and is also a "TD" mutation that has been shown to improve trimerization of soluble gp140s (9). I165L might alter packing of V2 on the trimer to improve accommodation of V2 bnAb. K169 has been associated with decreased risk of infection in the RV144 clinical trial (12, 62, 63). Antibodies were also isolated from RV144 vaccinees that bound to K169 and, although they only neutralized Tier 1 viruses, were capable of mediating ADCC against tier 2 isolates, which has suggested a mechanism for RV144 vaccine protection (64). We found that V169K increased Env recognition and MPN by multiple V2 bnAbs, which might be explained by the Lys side chain improving interactions with anionic, Tyr-sulfated CDR H3s of these antibodies (16, 21). Notably, the MPN of PGT145 was decreased by V169K, so some heterogeneity in V2 must exist with this mutant, perhaps due to interactions of K169 with surrounding glycosylation. PGT145 reportedly binds in a "straight-up-and-down" orientation and makes contact with all three gp120 protomers, in contrast to the asymmetric approach of PG9-type V2 bnAbs, which could make penetrating a stabilized trimer apex more difficult (54). However, PGDM1400 is a somatic variant of PGT145 that binds to the trimer in the same orientation as PGT145 (17), and its MPN is not reduced against CM-LK, so we speculate that the reduced PGT145 neutralization is due to effects of local and residual glycan heterogeneity that hinders PGT145 but that PGDM1400 can avoid. Virus containing a mixture of Comb-mut and CM-LK—which individually showed either PG9 or PGT145 partial neutralization—was 100% neutralized by a cocktail of the two antibodies, suggesting that glycosylation sites from adjacent protomers were modified and recognized independently.

We showed that the thermostability of ADA was increased by blocking complex glycosylation, e.g., using swainsonine, kifunensine, and GnTI$^{-/-}$ cells. The effects of glycosylation on protein stability can be difficult to predict. However, increasing glycosylation has boosted protein stability in other systems (65–67). Perhaps the untrimmed mannose residues left by glycosylation inhibitors stabilize Env through packing of the larger, more uniform mannose residues, or by reducing the favorability of unfolding by altering the entropy of water in the hydration shell over exposed hydrophobic protein patches similar to the mechanism by which polyethylene glycol modifications improve thermostability of proteins (68, 69). Whatever the mechanism, our results suggest that preventing the trimming of glycans may be a useful tool for increasing the functional thermostability of membrane Env immunogens.

BN-PAGE analysis showed that Comb-mut-LK trimers were recognized more efficiently and by a greater number of V2 bnAbs than Comb-mut and that the bnAb-Env association was improved further by chemical cross-linking. We note, too, that MPER and gp41 interface bnAbs 10E8, PGT151, and 35O22 potently neutralize Comb-mut-LKQ with high MPNs similar to those for Comb-mut (70), suggesting that this Env is relatively homogeneous throughout the trimer interfaces.

Will Env trimer stabilization help in eliciting bnAb? No immunizations with soluble trimers stable or otherwise have elicited significant bnAb responses so additional factors will most likely play a role (71, 72). Feng et al. showed recently that trimer stability correlated with elicitation of autologous nAbs against a few Envs (73). Unstable trimers are prone to shedding of gp120 (74), proteolysis (75) and antibody-mediated destabilization (51, 76), which may limit B cell responses against quaternary bnAb epitopes. Autologous nAbs have been associated with Envs that lack particular glycans

("glycan holes") including JR-FL, BG505, and CAP257 that lack glycans at N197, N241, and V5, respectively (77–79). Eliciting bnAbs may require B cells of specific germ line origins (80) and high levels of somatic hypermutation (81). In order to better inform strategies to elicit bnAbs (i.e., trigger relevant B cells, drive desired affinity maturation, and limit off-target responses), definition and control over Env trimer heterogeneity and stability will likely become more important.

MATERIALS AND METHODS

Plasmids and cell lines. Reagents obtained through the NIH AIDS Reagent Program included pSG3Δenv from J. Kappes and X. Wu (82), pLAI.2 from K. Peden (83), and TZM-bl cells from J. Kappes, X. Wu, and Tranzyme, Inc. (84). Plasmids pcDNA-ADA, pcDNA-Comb-mut, pLAI-ADA, and pLAI-Comb-mut were described previously (44). BG505 N332 env was synthesized using codon optimization and a tPA leader (GeneWiz) and subcloned into the vector, pLentiIII (ABM, Canada). HEK-293T cells were purchased from the American Type Culture Collection, and HEK-293S cells were kindly provided by H. G. Khorana (MIT).

Antibodies and antibody production. IgGs b12, PG9, PG16, PGT128, PGT145, PGDM1400, F425-B4e8, 2F5, VRC01, Z13e1, and 10E8 were produced in-house. Antibodies were produced starting with two plasmid DNAs, one containing a heavy chain and a other light chain, which were transiently transfected into 293F cells; IgG was purified from cell culture supernatant by protein A affinity chromatography, as previously described (85). For some early experiments, b12, PG9, PG16, PGT128, PGT145, and PGDM1400 were kindly provided by Dennis Burton (TSRI). CH01 was a gift from B. Haynes (Duke University), and VRC26.08 was provided by J. Mascola (VRC). 4E10 and 2G12 were purchased from Polymun Scientific (Austria). The antibodies 19b, 39F, and 17b were a gift from James Robinson (Tulane).

Env mutagenesis. Mutations were introduced into Env ADA and Comb-mut in pcDNA3.1 using a QuikChange kit (Agilent) according to the protocol provided. Plasmids were DNA sequence verified, transformed into NEB 5-alpha cells (New England BioLabs), and purified using a Maxiprep kit (Qiagen). Key mutants of Env were subcloned into the pLAI plasmid to produce infectious molecular clone (IMC) as previously described (86).

Virus production. Pseudotyped virus was produced using HEK-293T cells that were transiently transfected with Env plasmid DNA, the HIV-1 backbone plasmid, pSG3ΔEnv (82) and 25K polyethyleneimine, as previously described (86). In some cases, kifunensine and swainsonine were added to cells 30 min prior to transfection at 25 and 20 μM, respectively (4, 43). IMC was produced by the transient transfection of HEK-293T cells using pLAI-ADA, pLAI-Comb-mut, and cognate mutants. Cell culture supernatant was harvested 3 days posttransfection and centrifuged at 20,000 rpm to pellet the virus. Virions were resuspended in 100× phosphate-buffered saline and frozen at −80°C.

Infectivity and neutralization assays. Viral infectivity and neutralization assays were performed as described previously (86). Briefly, TZM-bl cells were seeded onto a 96-well plate in 100 μl of Dulbecco modified Eagle medium supplemented with fetal bovine serum, penicillin, streptomycin, and glutamine. Cells were incubated at 37°C for 24 h prior to addition of virus. Virus was coincubated with inhibitor at 37°C for 1 h prior to adding to TZM-bl cells. Virus neutralization was determined 48 h later by adding Bright-Glo (Promega) and measuring luciferase activity using a Synergy H1 plate reader (BioTek).

HIV-1 Env stability-of-function assay. Thermostability (T90) assays were performed as described previously (45). Briefly, pseudotyped virus was incubated at temperatures from 37°C to 57°C for 1 h on a Mastercycler PCR Gradient (Eppendorf). Virus aliquots were added to microwells containing TZM-bl cells. Infectivity was determined as above and plotted as a function of temperature. T90 values were interpolated as the temperature at which virus infectivity decreased by 90%.

BN-PAGE mobility shift and Western blotting. BN-PAGE mobility shift assays were performed as previously described (43, 44, 75). To measure Env trimer stability, virions were subjected to a heat gradient prior to electrophoresis. For gel mobility shift assays, IMCs were incubated with antibody at room temperature for 30 min. In some cases virus was cross-linked using BS^3 (Thermo) to prevent bound antibody from dissociating during the gel run. Virus was solubilized with 1% DDM and loaded onto a 3 to 12% gradient NativePAGE Bis-Tris gel (Invitrogen). Proteins were transferred onto a polyvinylidene difluoride membrane (Bio-Rad), probed using a cocktail of antibodies to gp120 (b12, 2G12, and F425-B4e8; 2 μg/ml each) and gp41 (4E10, Z13e1, and 2F5; 1 μg/ml each), and the blot was developed using ECL Plus substrate (Life Technologies).

ACKNOWLEDGMENTS

We thank Marisa Liu and Avery Normandin for technical assistance and Armando Stano for helpful discussions. We thank Dennis Burton (TSRI), Mark Connors (VRC), and John Mascola (VRC) for supplying antibody plasmids and Don Mosier (TSRI) for providing 5P12-RANTES-resistant mutants of HIV-1.

We acknowledge grant support from the National Institutes of Health (NIAID), R33 AI077381 and R01 AI098602, as well as the James B. Pendleton Charitable Trust.

REFERENCES

1. Burton DR, Hangartner L. 2016. Broadly neutralizing antibodies to HIV and their role in vaccine design. Annu Rev Immunol 34:635–659. https://doi.org/10.1146/annurev-immunol-041015-055515.
2. Burton DR, Ahmed R, Barouch DH, Butera ST, Crotty S, Godzik A, Kaufmann DE, McElrath MJ, Nussenzweig MC, Pulendran B, Scanlan CN, Schief WR, Silvestri G, Streeck H, Walker BD, Walker LM, Ward AB, Wilson IA, Wyatt R. 2012. A blueprint for HIV vaccine discovery. Cell Host Microbe 12:396–407. https://doi.org/10.1016/j.chom.2012.09.008.
3. Sanders RW, van Gils MJ, Derking R, Sok D, Ketas TJ, Burger JA, Ozorowski G, Cupo A, Simonich C, Goo L, Arendt H, Kim HJ, Lee JH, Pugach P, Williams M, Debnath G, Moldt B, van Breemen MJ, Isik G, Medina-Ramirez M, Back JW, Koff WC, Julien JP, Rakasz EG, Seaman MS, Guttman M, Lee KK, Klasse PJ, LaBranche C, Schief WR, Wilson IA, Overbaugh J, Burton DR, Ward AB, Montefiori DC, Dean H, Moore JP. 2015. HIV-1 VACCINES: HIV-1 neutralizing antibodies induced by native-like envelope trimers. Science 349:aac4223. https://doi.org/10.1126/science.aac4223.
4. Doores KJ, Burton DR. 2010. Variable loop glycan dependency of the broad and potent HIV-1-neutralizing antibodies PG9 and PG16. J Virol 84:10510–10521. https://doi.org/10.1128/JVI.00552-10.
5. McCoy LE, Falkowska E, Doores KJ, Le K, Sok D, van Gils MJ, Euler Z, Burger JA, Seaman MS, Sanders RW, Schuitemaker H, Poignard P, Wrin T, Burton DR. 2015. Incomplete neutralization and deviation from sigmoidal neutralization curves for HIV broadly neutralizing monoclonal antibodies. PLoS Pathog 11:e1005110. https://doi.org/10.1371/journal.ppat.1005110.
6. McGuire AT, Glenn JA, Lippy A, Stamatatos L. 2014. Diverse recombinant HIV-1 Envs fail to activate B cells expressing the germ line B cell receptors of the broadly neutralizing anti-HIV-1 antibodies PG9 and 447-52D. J Virol 88:2645–2657. https://doi.org/10.1128/JVI.03228-13.
7. Lyumkis D, Julien JP, de Val N, Cupo A, Potter CS, Klasse PJ, Burton DR, Sanders RW, Moore JP, Carragher B, Wilson IA, Ward AB. 2013. Cryo-EM structure of a fully glycosylated soluble cleaved HIV-1 envelope trimer. Science 342:1484–1490. https://doi.org/10.1126/science.1245627.
8. Julien JP, Cupo A, Sok D, Stanfield RL, Lyumkis D, Deller MC, Klasse PJ, Burton DR, Sanders RW, Moore JP, Ward AB, Wilson IA. 2013. Crystal structure of a soluble cleaved HIV-1 envelope trimer. Science 342:1477–1483. https://doi.org/10.1126/science.1245625.
9. Guenaga J, Dubrovskaya V, de Val N, Sharma SK, Carrette B, Ward AB, Wyatt RT. 2015. Structure-guided redesign increases the propensity of HIV Env to generate highly stable soluble trimers. J Virol 90:2806–2817. https://doi.org/10.1128/JVI.02652-15.
10. Sharma SK, de Val N, Bale S, Guenaga J, Tran K, Feng Y, Dubrovskaya V, Ward AB, Wyatt RT. 2015. Cleavage-independent HIV-1 Env trimers engineered as soluble native spike mimetics for vaccine design. Cell Rep 11:539–550. https://doi.org/10.1016/j.celrep.2015.03.047.
11. Zolla-Pazner S, deCamp A, Gilbert PB, Williams C, Yates NL, Williams WT, Howington R, Fong Y, Morris DE, Soderberg KA, Irene C, Reichman C, Pinter A, Parks R, Pitisuttithum P, Kaewkungwal J, Rerks-Ngarm S, Nitayaphan S, Andrews C, O'Connell RJ, Yang ZY, Nabel GJ, Kim JH, Michael NL, Montefiori DC, Liao HX, Haynes BF, Tomaras GD. 2014. Vaccine-induced IgG antibodies to V1V2 regions of multiple HIV-1 subtypes correlate with decreased risk of HIV-1 infection. PLoS One 9:e87572. https://doi.org/10.1371/journal.pone.0087572.
12. Karasavvas N, Billings E, Rao M, Williams C, Zolla-Pazner S, Bailer RT, Koup RA, Madnote S, Arworn D, Shen X, Tomaras GD, Currier JR, Jiang M, Magaret C, Andrews C, Gottardo R, Gilbert P, Cardozo TJ, Rerks-Ngarm S, Nitayaphan S, Pitisuttithum P, Kaewkungwal J, Paris R, Greene K, Gao H, Gurunathan S, Tartaglia J, Sinangil F, Korber BT, Montefiori DC, Mascola JR, Robb ML, Haynes BF, Ngauy V, Michael NL, Kim JH, de Souza MS, Collaboration MT. 2012. The Thai Phase III HIV Type 1 Vaccine Trial (RV144) regimen induces antibodies that target conserved regions within the V2 loop of gp120. AIDS Res Hum Retroviruses 28:1444–1457. https://doi.org/10.1089/aid.2012.0103.
13. Roederer M, Keele BF, Schmidt SD, Mason RD, Welles HC, Fischer W, Labranche C, Foulds KE, Louder MK, Yang ZY, Todd JP, Buzby AP, Mach LV, Shen L, Seaton KE, Ward BM, Bailer RT, Gottardo R, Gu W, Ferrari G, Alam SM, Denny TN, Montefiori DC, Tomaras GD, Korber BT, Nason MC, Seder RA, Koup RA, Letvin NL, Rao SS, Nabel GJ, Mascola JR. 2014. Immunological and virological mechanisms of vaccine-mediated protection against SIV and HIV. Nature 505:502–508. https://doi.org/10.1038/nature12893.
14. Walker LM, Phogat SK, Chan-Hui PY, Wagner D, Phung P, Goss JL, Wrin T, Simek MD, Fling S, Mitcham JL, Lehrman JK, Priddy FH, Olsen OA, Frey SM, Hammond PW, Protocol GPI, Kaminsky S, Zamb T, Moyle M, Koff WC, Poignard P, Burton DR. 2009. Broad and potent neutralizing antibodies from an African donor reveal a new HIV-1 vaccine target. Science 326:285–289. https://doi.org/10.1126/science.1178746.
15. Walker LM, Huber M, Doores KJ, Falkowska E, Pejchal R, Julien JP, Wang SK, Ramos A, Chan-Hui PY, Moyle M, Mitcham JL, Hammond PW, Olsen OA, Phung P, Fling S, Wong CH, Phogat S, Wrin T, Simek MD, Protocol GPI, Koff WC, Wilson IA, Burton DR, Poignard P. 2011. Broad neutralization coverage of HIV by multiple highly potent antibodies. Nature 477:466–470. https://doi.org/10.1038/nature10373.
16. Doria-Rose NA, Schramm CA, Gorman J, Moore PL, Bhiman JN, DeKosky BJ, Ernandes MJ, Georgiev IS, Kim HJ, Pancera M, Staupe RP, Altae-Tran HR, Bailer RT, Crooks ET, Cupo A, Druz A, Garrett NJ, Hoi KH, Kong R, Louder MK, Longo NS, McKee K, Nonyane M, O'Dell S, Roark RS, Rudicell RS, Schmidt SD, Sheward DJ, Soto C, Wibmer CK, Yang Y, Zhang Z, Program NCS, Mullikin JC, Binley JM, Sanders RW, Wilson IA, Moore JP, Ward AB, Georgiou G, Williamson C, Abdool Karim SS, Morris L, Kwong PD, Shapiro L, Mascola JR. 2014. Developmental pathway for potent V1V2-directed HIV-neutralizing antibodies. Nature 509:55–62. https://doi.org/10.1038/nature13036.
17. Sok D, van Gils MJ, Pauthner M, Julien JP, Saye-Francisco KL, Hsueh J, Briney B, Lee JH, Le KM, Lee PS, Hua Y, Seaman MS, Moore JP, Ward AB, Wilson IA, Sanders RW, Burton DR. 2014. Recombinant HIV envelope trimer selects for quaternary-dependent antibodies targeting the trimer apex. Proc Natl Acad Sci U S A 111:17624–17629. https://doi.org/10.1073/pnas.1415789111.
18. Ringe R, Phogat S, Bhattacharya J. 2012. Subtle alteration of residues including N-linked glycans in V2 loop modulate HIV-1 neutralization by PG9 and PG16 monoclonal antibodies. Virology 426:34–41. https://doi.org/10.1016/j.virol.2012.01.011.
19. Thenin S, Roch E, Samleerat T, Moreau T, Chaillon A, Moreau A, Barin F, Braibant M. 2012. Naturally occurring substitutions of conserved residues in human immunodeficiency virus type 1 variants of different clades are involved in PG9 and PG16 resistance to neutralization. J Gen Virol 93:1495–1505. https://doi.org/10.1099/vir.0.042614-0.
20. Doria-Rose NA, Georgiev I, O'Dell S, Chuang GY, Staupe RP, McLellan JS, Gorman J, Pancera M, Bonsignori M, Haynes BF, Burton DR, Koff WC, Kwong PD, Mascola JR. 2012. A short segment of the HIV-1 gp120 V1/V2 region is a major determinant of resistance to V1/V2 neutralizing antibodies. J Virol 86:8319–8323. https://doi.org/10.1128/JVI.00696-12.
21. McLellan JS, Pancera M, Carrico C, Gorman J, Julien JP, Khayat R, Louder R, Pejchal R, Sastry M, Dai K, O'Dell S, Patel N, Shahzad-ul-Hussan S, Yang Y, Zhang B, Zhou T, Zhu J, Boyington JC, Chuang GY, Diwanji D, Georgiev I, Kwon YD, Lee D, Louder MK, Moquin S, Schmidt SD, Yang ZY, Bonsignori M, Crump JA, Kapiga SH, Sam NE, Haynes BF, Burton DR, Koff WC, Walker LM, Phogat S, Wyatt R, Orwenyo J, Wang LX, Arthos J, Bewley CA, Mascola JR, Nabel GJ, Schief WR, Ward AB, Wilson IA, Kwong PD. 2011. Structure of HIV-1 gp120 V1/V2 domain with broadly neutralizing antibody PG9. Nature 480:336–343. https://doi.org/10.1038/nature10696.
22. Bonsignori M, Hwang KK, Chen X, Tsao CY, Morris L, Gray E, Marshall DJ, Crump JA, Kapiga SH, Sam NE, Sinangil F, Pancera M, Yongping Y, Zhang B, Zhu J, Kwong PD, O'Dell S, Mascola JR, Wu L, Nabel GJ, Phogat S, Seaman MS, Whitesides JF, Moody MA, Kelsoe G, Yang X, Sodroski J, Shaw GM, Montefiori DC, Kepler TB, Tomaras GD, Alam SM, Liao HX, Haynes BF. 2011. Analysis of a clonal lineage of HIV-1 envelope V2/V3 conformational epitope-specific broadly neutralizing antibodies and their inferred unmutated common ancestors. J Virol 85:9998–10009. https://doi.org/10.1128/JVI.05045-11.
23. Davenport TM, Friend D, Ellingson K, Xu H, Caldwell Z, Sellhorn G, Kraft Z, Strong RK, Stamatatos L. 2011. Binding interactions between soluble HIV envelope glycoproteins and quaternary-structure-specific monoclonal antibodies PG9 and PG16. J Virol 85:7095–7107. https://doi.org/10.1128/JVI.00411-11.
24. Julien JP, Lee JH, Cupo A, Murin CD, Derking R, Hoffenberg S, Caulfield MJ, King CR, Marozsan AJ, Klasse PJ, Sanders RW, Moore JP, Wilson IA, Ward AB. 2013. Asymmetric recognition of the HIV-1 trimer by broadly

neutralizing antibody PG9. Proc Natl Acad Sci U S A 110:4351–4356. https://doi.org/10.1073/pnas.1217537110.
25. Pancera M, McLellan JS, Wu X, Zhu J, Changela A, Schmidt SD, Yang Y, Zhou T, Phogat S, Mascola JR, Kwong PD. 2010. Crystal structure of PG16 and chimeric dissection with somatically related PG9: structure-function analysis of two quaternary-specific antibodies that effectively neutralize HIV-1. J Virol 84:8098–8110. https://doi.org/10.1128/JVI.00966-10.
26. Pejchal R, Walker LM, Stanfield RL, Phogat SK, Koff WC, Poignard P, Burton DR, Wilson IA. 2010. Structure and function of broadly reactive antibody PG16 reveal an H3 subdomain that mediates potent neutralization of HIV-1. Proc Natl Acad Sci U S A 107:11483–11488. https://doi.org/10.1073/pnas.1004600107.
27. O'Rourke SM, Sutthent R, Phung P, Mesa KA, Frigon NL, To B, Horthongkham N, Limoli K, Wrin T, Berman PW. 2015. Glycans flanking the hypervariable connecting peptide between the A and B strands of the V1/V2 domain of HIV-1 gp120 confer resistance to antibodies that neutralize CRF01_AE viruses. PLoS One 10:e0119608. https://doi.org/10.1371/journal.pone.0119608.
28. Pancera M, Shahzad-Ul-Hussan S, Doria-Rose NA, McLellan JS, Bailer RT, Dai K, Loesgen S, Louder MK, Staupe RP, Yang Y, Zhang B, Parks R, Eudailey J, Lloyd KE, Blinn J, Alam SM, Haynes BF, Amin MN, Wang LX, Burton DR, Koff WC, Nabel GJ, Mascola JR, Bewley CA, Kwong PD. 2013. Structural basis for diverse N-glycan recognition by HIV-1-neutralizing V1-V2-directed antibody PG16. Nat Struct Mol Biol 20:804–813. https://doi.org/10.1038/nsmb.2600.
29. Amin MN, McLellan JS, Huang W, Orwenyo J, Burton DR, Koff WC, Kwong PD, Wang LX. 2013. Synthetic glycopeptides reveal the glycan specificity of HIV-neutralizing antibodies. Nat Chem Biol 9:521–526. https://doi.org/10.1038/nchembio.1288.
30. Morales JF, Morin TJ, Yu B, Tatsuno GP, O'Rourke SM, Theolis R, Jr, Mesa KA, Berman PW. 2014. HIV-1 envelope proteins and V1/V2 domain scaffolds with mannose-5 to improve the magnitude and quality of protective antibody responses to HIV-1. J Biol Chem 289:20526–20542. https://doi.org/10.1074/jbc.M114.554089.
31. Zolla-Pazner S, Cohen SS, Boyd D, Kong XP, Seaman M, Nussenzweig M, Klein F, Overbaugh J, Totrov M. 2015. Structure/function studies involving the V3 region of the HIV-1 envelope delineate multiple factors that affect neutralization sensitivity. J Virol 90:636–649. https://doi.org/10.1128/JVI.01645-15.
32. Pantophlet R, Wrin T, Cavacini LA, Robinson JE, Burton DR. 2008. Neutralizing activity of antibodies to the V3 loop region of HIV-1 gp120 relative to their epitope fine specificity. Virology 381:251–260. https://doi.org/10.1016/j.virol.2008.08.032.
33. Sok D, Doores KJ, Briney B, Le KM, Saye-Francisco KL, Ramos A, Kulp DW, Julien JP, Menis S, Wickramasinghe L, Seaman MS, Schief WR, Wilson IA, Poignard P, Burton DR. 2014. Promiscuous glycan site recognition by antibodies to the high-mannose patch of gp120 broadens neutralization of HIV. Sci Transl Med 6:236ra263. https://doi.org/10.1126/scitranslmed.3008104.
34. Pejchal R, Doores KJ, Walker LM, Khayat R, Huang PS, Wang SK, Stanfield RL, Julien JP, Ramos A, Crispin M, Depetris R, Katpally U, Marozsan A, Cupo A, Maloveste S, Liu Y, McBride R, Ito Y, Sanders RW, Ogohara C, Paulson JC, Feizi T, Scanlan CN, Wong CH, Moore JP, Olson WC, Ward AB, Poignard P, Schief WR, Burton DR, Wilson IA. 2011. A potent and broad neutralizing antibody recognizes and penetrates the HIV glycan shield. Science 334:1097–1103. https://doi.org/10.1126/science.1213256.
35. de Taeye SW, Ozorowski G, Torrents de la Pena A, Guttman M, Julien JP, van den Kerkhof TL, Burger JA, Pritchard LK, Pugach P, Yasmeen A, Crampton J, Hu J, Bontjer I, Torres JL, Arendt H, DeStefano J, Koff WC, Schuitemaker H, Eggink D, Berkhout B, Dean H, LaBranche C, Crotty S, Crispin M, Montefiori DC, Klasse PJ, Lee KK, Moore JP, Wilson IA, Ward AB, Sanders RW. 2015. Immunogenicity of stabilized HIV-1 envelope trimers with reduced exposure of non-neutralizing epitopes. Cell 163:1702–1715. https://doi.org/10.1016/j.cell.2015.11.056.
36. Kwon YD, Pancera M, Acharya P, Georgiev IS, Crooks ET, Gorman J, Joyce MG, Guttman M, Ma X, Narpala S, Soto C, Terry DS, Yang Y, Zhou T, Ahlsen G, Bailer RT, Chambers M, Chuang GY, Doria-Rose NA, Druz A, Hallen MA, Harned A, Kirys T, Louder MK, O'Dell S, Ofek G, Osawa K, Prabhakaran M, Sastry M, Stewart-Jones GB, Stuckey J, Thomas PV, Tittley T, Williams C, Zhang B, Zhao H, Zhou Z, Donald BR, Lee LK, Zolla-Pazner S, Baxa U, Schon A, Freire E, Shapiro L, Lee KK, Arthos J, Munro JB, Blanchard SC, Mothes W, Binley JM, et al. 2015. Crystal structure, conformational fixation and entry-related interactions of mature ligand-free HIV-1 Env. Nat Struct Mol Biol 22:522–531. https://doi.org/10.1038/nsmb.3051.
37. Leaman DP, Lee JH, Ward AB, Zwick MB. 2015. Immunogenic display of purified chemically cross-linked HIV-1 spikes. J Virol 89:6725–6745. https://doi.org/10.1128/JVI.03738-14.
38. Shental-Bechor D, Levy Y. 2008. Effect of glycosylation on protein folding: a close look at thermodynamic stabilization. Proc Natl Acad Sci U S A 105:8256–8261. https://doi.org/10.1073/pnas.0801340105.
39. Land A, Braakman I. 2001. Folding of the human immunodeficiency virus type 1 envelope glycoprotein in the endoplasmic reticulum. Biochimie 83:783–790. https://doi.org/10.1016/S0300-9084(01)01314-1.
40. Go EP, Irungu J, Zhang Y, Dalpathado DS, Liao HX, Sutherland LL, Alam SM, Haynes BF, Desaire H. 2008. Glycosylation site-specific analysis of HIV envelope proteins (JR-FL and CON-S) reveals major differences in glycosylation site occupancy, glycoform profiles, and antigenic epitopes' accessibility. J Proteome Res 7:1660–1674. https://doi.org/10.1021/pr7006957.
41. Crispin M, Doores KJ. 2015. Targeting host-derived glycans on enveloped viruses for antibody-based vaccine design. Curr Opin Virol 11:63–69. https://doi.org/10.1016/j.coviro.2015.02.002.
42. Chikere K, Webb NE, Chou T, Borm K, Sterjovski J, Gorry PR, Lee B. 2014. Distinct HIV-1 entry phenotypes are associated with transmission, subtype specificity, and resistance to broadly neutralizing antibodies. Retrovirology 11:48. https://doi.org/10.1186/1742-4690-11-48.
43. Kim AS, Leaman DP, Zwick MB. 2014. Antibody to gp41 MPER alters functional properties of HIV-1 Env without complete neutralization. PLoS Pathog 10:e1004271. https://doi.org/10.1371/journal.ppat.1004271.
44. Leaman DP, Zwick MB. 2013. Increased functional stability and homogeneity of viral envelope spikes through directed evolution. PLoS Pathog 9:e1003184. https://doi.org/10.1371/journal.ppat.1003184.
45. Agrawal N, Leaman DP, Rowcliffe E, Kinkead H, Nohria R, Akagi J, Bauer K, Du SX, Whalen RG, Burton DR, Zwick MB. 2011. Functional stability of unliganded envelope glycoprotein spikes among isolates of human immunodeficiency virus type 1 (HIV-1). PLoS One 6:e21339. https://doi.org/10.1371/journal.pone.0021339.
46. Murray EJ, Leaman DP, Pawa N, Perkins H, Pickford C, Perros M, Zwick MB, Butler SL. 2010. A low-molecular-weight entry inhibitor of both CCR5- and CXCR4-tropic strains of human immunodeficiency virus type 1 targets a novel site on gp41. J Virol 84:7288–7299. https://doi.org/10.1128/JVI.00535-10.
47. Nedellec R, Coetzer M, Lederman MM, Offord RE, Hartley O, Mosier DE. 2011. Resistance to the CCR5 inhibitor 5P12-RANTES requires a difficult evolution from CCR5 to CXCR4 coreceptor use. PLoS One 6:e22020. https://doi.org/10.1371/journal.pone.0022020.
48. Doria-Rose NA, Bhiman JN, Roark RS, Schramm CA, Gorman J, Chuang GY, Pancera M, Cale EM, Ernandes MJ, Louder MK, Asokan M, Bailer RT, Druz A, Fraschilla IR, Garrett NJ, Jarosinski M, Lynch RM, McKee K, O'Dell S, Pegu A, Schmidt SD, Staupe RP, Sutton MS, Wang K, Wibmer CK, Haynes BF, Abdool-Karim S, Shapiro L, Kwong PD, Moore PL, Morris L, Mascola JR. 2015. New member of the V1V2-directed CAP256-VRC26 lineage that shows increased breadth and exceptional potency. J Virol 90:76–91. https://doi.org/10.1128/JVI.01791-15.
49. Falkowska E, Le KM, Ramos A, Doores KJ, Lee JH, Blattner C, Ramirez A, Derking R, van Gils MJ, Liang CH, McBride R, von Bredow B, Shivatare SS, Wu CY, Chan-Hui PY, Liu Y, Feizi T, Zwick MB, Koff WC, Seaman MS, Swiderek K, Moore JP, Evans D, Paulson JC, Wong CH, Ward AB, Wilson IA, Sanders RW, Poignard P, Burton DR. 2014. Broadly neutralizing HIV antibodies define a glycan-dependent epitope on the prefusion conformation of gp41 on cleaved envelope trimers. Immunity 40:657–668. https://doi.org/10.1016/j.immuni.2014.04.009.
50. Huang J, Kang BH, Pancera M, Lee JH, Tong T, Feng Y, Georgiev IS, Chuang GY, Druz A, Doria-Rose NA, Laub L, Sliepen K, van Gils MJ, de la Pena AT, Derking R, Klasse PJ, Migueles SA, Bailer RT, Alam M, Pugach P, Haynes BF, Wyatt RT, Sanders RW, Binley JM, Ward AB, Mascola JR, Kwong PD, Connors M. 2014. Broad and potent HIV-1 neutralization by a human antibody that binds the gp41-gp120 interface. Nature 515:138–142. https://doi.org/10.1038/nature13601.
51. Lee JH, Leaman DP, Kim AS, Torrents de la Pena A, Sliepen K, Yasmeen A, Derking R, Ramos A, de Taeye SW, Ozorowski G, Klein F, Burton DR, Nussenzweig MC, Poignard P, Moore JP, Klasse PJ, Sanders RW, Zwick MB, Wilson IA, Ward AB. 2015. Antibodies to a conformational epitope on gp41 neutralize HIV-1 by destabilizing the Env spike. Nat Commun 6:8167. https://doi.org/10.1038/ncomms9167.
52. Herschhorn A, Ma X, Gu C, Ventura JD, Castillo-Menendez L, Melillo B, Terry DS, Smith AB 3rd, Blanchard SC, Munro JB, Mothes W, Finzi A,

Sodroski J. 2016. Release of gp120 restraints leads to an entry-competent intermediate state of the HIV-1 envelope glycoproteins. mBio 7:e01598-16. https://doi.org/10.1128/mBio.01598-16.
53. Scanlan CN, Ritchie GE, Baruah K, Crispin M, Harvey DJ, Singer BB, Lucka L, Wormald MR, Wentworth P, Jr, Zitzmann N, Rudd PM, Burton DR, Dwek RA. 2007. Inhibition of mammalian glycan biosynthesis produces non-self antigens for a broadly neutralising, HIV-1-specific antibody. J Mol Biol 372:16–22. https://doi.org/10.1016/j.jmb.2007.06.027.
54. Lee JH, Andrabi R, Su CY, Yasmeen A, Julien JP, Kong L, Wu NC, McBride R, Sok D, Pauthner M, Cottrell CA, Nieusma T, Blattner C, Paulson JC, Klasse PJ, Wilson IA, Burton DR, Ward AB. 2017. A broadly neutralizing antibody targets the dynamic HIV envelope trimer apex via a long, rigidified, and anionic beta-hairpin structure. Immunity 46:690–702. https://doi.org/10.1016/j.immuni.2017.03.017.
55. Upadhyay C, Mayr LM, Zhang J, Kumar R, Gorny MK, Nadas A, Zolla-Pazner S, Hioe CE. 2014. Distinct mechanisms regulate exposure of neutralizing epitopes in the V2 and V3 loops of HIV-1 envelope. J Virol 88:12853–12865. https://doi.org/10.1128/JVI.02125-14.
56. Binley JM, Ban YE, Crooks ET, Eggink D, Osawa K, Schief WR, Sanders RW. 2010. Role of complex carbohydrates in human immunodeficiency virus type 1 infection and resistance to antibody neutralization. J Virol 84:5637–5655. https://doi.org/10.1128/JVI.00105-10.
57. Zolla-Pazner S, Zhong P, Revesz K, Volsky B, Williams C, Nyambi P, Gorny MK. 2004. The cross-clade neutralizing activity of a human monoclonal antibody is determined by the GPGR V3 motif of HIV type 1. AIDS Res Hum Retroviruses 20:1254–1258. https://doi.org/10.1089/aid.2004.20.1254.
58. Pancera M, Zhou T, Druz A, Georgiev IS, Soto C, Gorman J, Huang J, Acharya P, Chuang GY, Ofek G, Stewart-Jones GB, Stuckey J, Bailer RT, Joyce MG, Louder MK, Tumba N, Yang Y, Zhang B, Cohen MS, Haynes BF, Mascola JR, Morris L, Munro JB, Blanchard SC, Mothes W, Connors M, Kwong PD. 2014. Structure and immune recognition of trimeric pre-fusion HIV-1 Env. Nature 514:455–461. https://doi.org/10.1038/nature13808.
59. Eggink D, de Taeye SW, Bontjer I, Klasse PJ, Langedijk JP, Berkhout B, Sanders RW. 2016. HIV-1 escape from a peptidic anchor inhibitor through stabilization of the envelope glycoprotein spike. J Virol 90:10587–10599. https://doi.org/10.1128/JVI.01616-16.
60. Zhuang M, Wang W, De Feo CJ, Vassell R, Weiss CD. 2012. Trimeric, coiled-coil extension on peptide fusion inhibitor of HIV-1 influences selection of resistance pathways. J Biol Chem 287:8297–8309. https://doi.org/10.1074/jbc.M111.324483.
61. Beauparlant D, Rusert P, Magnus C, Kadelka C, Weber J, Uhr T, Zagordi O, Oberle C, Duenas-Decamp MJ, Clapham PR, Metzner KJ, Gunthard HF, Trkola A. 2017. Delineating CD4 dependency of HIV-1: adaptation to infect low level CD4 expressing target cells widens cellular tropism but severely impacts on envelope functionality. PLoS Pathog 13:e1006255. https://doi.org/10.1371/journal.ppat.1006255.
62. Haynes BF, Gilbert PB, McElrath MJ, Zolla-Pazner S, Tomaras GD, Alam SM, Evans DT, Montefiori DC, Karnasuta C, Sutthent R, Liao HX, DeVico AL, Lewis GK, Williams C, Pinter A, Fong Y, Janes H, DeCamp A, Huang Y, Rao M, Billings E, Karasavvas N, Robb ML, Ngauy V, de Souza MS, Paris R, Ferrari G, Bailer RT, Soderberg KA, Andrews C, Berman PW, Frahm N, De Rosa SC, Alpert MD, Yates NL, Shen X, Koup RA, Pitisuttithum P, Kaewkungwal J, Nitayaphan S, Rerks-Ngarm S, Michael NL, Kim JH. 2012. Immune-correlates analysis of an HIV-1 vaccine efficacy trial. N Engl J Med 366:1275–1286. https://doi.org/10.1056/NEJMoa1113425.
63. Rolland M, Edlefsen PT, Larsen BB, Tovanabutra S, Sanders-Buell E, Hertz T, deCamp AC, Carrico C, Menis S, Magaret CA, Ahmed H, Juraska M, Chen L, Konopa P, Nariya S, Stoddard JN, Wong K, Zhao H, Deng W, Maust BS, Bose M, Howell S, Bates A, Lazzaro M, O'Sullivan A, Lei E, Bradfield A, Ibitamuno G, Assawadarachai V, O'Connell RJ, deSouza MS, Nitayaphan S, Rerks-Ngarm S, Robb ML, McLellan JS, Georgiev I, Kwong PD, Carlson JM, Michael NL, Schief WR, Gilbert PB, Mullins JI, Kim JH. 2012. Increased HIV-1 vaccine efficacy against viruses with genetic signatures in Env V2. Nature 490:417–420. https://doi.org/10.1038/nature11519.
64. Liao HX, Bonsignori M, Alam SM, McLellan JS, Tomaras GD, Moody MA, Kozink DM, Hwang KK, Chen X, Tsao CY, Liu P, Lu X, Parks RJ, Montefiori DC, Ferrari G, Pollara J, Rao M, Peachman KK, Santra S, Letvin NL, Karasavvas N, Yang ZY, Dai K, Pancera M, Gorman J, Wiehe K, Nicely NI, Rerks-Ngarm S, Nitayaphan S, Kaewkungwal J, Pitisuttithum P, Tartaglia J, Sinangil F, Kim JH, Michael NL, Kepler TB, Kwong PD, Mascola JR, Nabel GJ, Pinter A, Zolla-Pazner S, Haynes BF. 2013. Vaccine induction of antibodies against a structurally heterogeneous site of immune pressure within HIV-1 envelope protein variable regions 1 and 2. Immunity 38:176–186. https://doi.org/10.1016/j.immuni.2012.11.011.
65. Sola RJ, Al-Azzam W, Griebenow K. 2006. Engineering of protein thermodynamic, kinetic, and colloidal stability: chemical glycosylation with monofunctionally activated glycans. Biotechnol Bioeng 94:1072–1079. https://doi.org/10.1002/bit.20933.
66. Broersen K, Voragen AG, Hamer RJ, De Jongh HH. 2004. Glycoforms of beta-lactoglobulin with improved thermostability and preserved structural packing. Biotechnol Bioeng 86:78–87. https://doi.org/10.1002/bit.20030.
67. van Teeffelen AM, Broersen K, de Jongh HH. 2005. Glucosylation of beta-lactoglobulin lowers the heat capacity change of unfolding; a unique way to affect protein thermodynamics. Protein Sci 14:2187–2194. https://doi.org/10.1110/ps.051405005.
68. Rawat S, Raman Suri C, Sahoo DK. 2010. Molecular mechanism of polyethylene glycol mediated stabilization of protein. Biochem Biophys Res Commun 392:561–566. https://doi.org/10.1016/j.bbrc.2010.01.067.
69. Lawrence PB, Gavrilov Y, Matthews SS, Langlois MI, Shental-Bechor D, Greenblatt HM, Pandey BK, Smith MS, Paxman R, Torgerson CD, Merrell JP, Ritz CC, Prigozhin MB, Levy Y, Price JL. 2014. Criteria for selecting PEGylation sites on proteins for higher thermodynamic and proteolytic stability. J Am Chem Soc 136:17547–17560. https://doi.org/10.1021/ja5095183.
70. Stano A, Leaman DP, Kim AS, Zhang L, Autin L, Ingale J, Gift SK, Truong J, Wyatt RT, Olson AJ, Zwick MB. 2017. Dense array of spikes on HIV-1 virion particles. J Virol 91:415–417. https://doi.org/10.1128/JVI.00415-17.
71. Hu JK, Crampton JC, Cupo A, Ketas T, van Gils MJ, Sliepen K, de Taeye SW, Sok D, Ozorowski G, Deresa I, Stanfield R, Ward AB, Burton DR, Klasse PJ, Sanders RW, Moore JP, Crotty S. 2015. Murine antibody responses to cleaved soluble HIV-1 envelope trimers are highly restricted in specificity. J Virol 89:10383–10398. https://doi.org/10.1128/JVI.01653-15.
72. McGee K, Haim H, Korioth-Schmitz B, Espy N, Javanbakht H, Letvin N, Sodroski J. 2014. The selection of low envelope glycoprotein reactivity to soluble CD4 and cold during simian-human immunodeficiency virus infection of rhesus macaques. J Virol 88:21–40. https://doi.org/10.1128/JVI.01558-13.
73. Feng Y, Tran K, Bale S, Kumar S, Guenaga J, Wilson R, de Val N, Arendt H, DeStefano J, Ward AB, Wyatt RT. 2016. Thermostability of well-ordered HIV spikes correlates with the elicitation of autologous tier 2 neutralizing antibodies. PLoS Pathog 12:e1005767. https://doi.org/10.1371/journal.ppat.1005767.
74. Moore JP, McKeating JA, Weiss RA, Sattentau QJ. 1990. Dissociation of gp120 from HIV-1 virions induced by soluble CD4. Science 250:1139–1142. https://doi.org/10.1126/science.2251501.
75. Crooks ET, Tong T, Osawa K, Binley JM. 2011. Enzyme digests eliminate nonfunctional Env from HIV-1 particle surfaces, leaving native Env trimers intact and viral infectivity unaffected. J Virol 85:5825–5839. https://doi.org/10.1128/JVI.00154-11.
76. Ruprecht CR, Krarup A, Reynell L, Mann AM, Brandenberg OF, Berlinger L, Abela IA, Regoes RR, Gunthard HF, Rusert P, Trkola A. 2011. MPER-specific antibodies induce gp120 shedding and irreversibly neutralize HIV-1. J Exp Med 208:439–454. https://doi.org/10.1084/jem.20101907.
77. Crooks ET, Tong T, Chakrabarti B, Narayan K, Georgiev IS, Menis S, Huang X, Kulp D, Osawa K, Muranaka J, Stewart-Jones G, Destefano J, O'Dell S, LaBranche C, Robinson JE, Montefiori DC, McKee K, Du SX, Doria-Rose N, Kwong PD, Mascola JR, Zhu P, Schief WR, Wyatt RT, Whalen RG, Binley JM. 2015. Vaccine-Elicited Tier 2 HIV-1 Neutralizing antibodies bind to quaternary epitopes involving glycan-deficient patches proximal to the CD4 binding site. PLoS Pathog 11:e1004932. https://doi.org/10.1371/journal.ppat.1004932.
78. McCoy LE, van Gils MJ, Ozorowski G, Messmer T, Briney B, Voss JE, Kulp DW, Macauley MS, Sok D, Pauthner M, Menis S, Cottrell CA, Torres JL, Hsueh J, Schief WR, Wilson IA, Ward AB, Sanders RW, Burton DR. 2016. Holes in the glycan shield of the native HIV envelope are a target of trimer-elicited neutralizing antibodies. Cell Rep 16:2327–2338. https://doi.org/10.1016/j.celrep.2016.07.074.
79. Wibmer CK, Gorman J, Anthony CS, Mkhize NN, Druz A, York T, Schmidt SD, Labuschagne P, Louder MK, Bailer RT, Abdool Karim SS, Mascola JR, Williamson C, Moore PL, Kwong PD, Morris L. 2016. Structure of an N276-dependent HIV-1 neutralizing antibody targeting a rare V5 glycan hole adjacent to the CD4 binding site. J Virol 90:10220–10235. https://doi.org/10.1128/JVI.01357-16.
80. Stamatatos L, Pancera M, McGuire AT. 2017. Germline-targeting immunogens. Immunol Rev 275:203–216. https://doi.org/10.1111/imr.12483.
81. Andrabi R, Voss JE, Liang CH, Briney B, McCoy LE, Wu CY, Wong CH,

Poignard P, Burton DR. 2015. Identification of common features in prototype broadly neutralizing antibodies to HIV envelope V2 apex to facilitate vaccine design. Immunity 43:959–973. https://doi.org/10.1016/j.immuni.2015.10.014.
82. Wei X, Decker JM, Wang S, Hui H, Kappes JC, Wu X, Salazar-Gonzalez JF, Salazar MG, Kilby JM, Saag MS, Komarova NL, Nowak MA, Hahn BH, Kwong PD, Shaw GM. 2003. Antibody neutralization and escape by HIV-1. Nature 422:307–312. https://doi.org/10.1038/nature01470.
83. Peden K, Emerman M, Montagnier L. 1991. Changes in growth properties on passage in tissue culture of viruses derived from infectious molecular clones of HIV-1LAI, HIV-1MAL, and HIV-1ELI. Virology 185:661–672. https://doi.org/10.1016/0042-6822(91)90537-L.
84. Platt EJ, Wehrly K, Kuhmann SE, Chesebro B, Kabat D. 1998. Effects of CCR5 and CD4 cell surface concentrations on infections by macrophagetropic isolates of human immunodeficiency virus type 1. J Virol 72:2855–2864.
85. Nelson JD, Brunel FM, Jensen R, Crooks ET, Cardoso RM, Wang M, Hessell A, Wilson IA, Binley JM, Dawson PE, Burton DR, Zwick MB. 2007. An affinity-enhanced neutralizing antibody against the membrane-proximal external region of human immunodeficiency virus type 1 gp41 recognizes an epitope between those of 2F5 and 4E10. J Virol 81:4033–4043. https://doi.org/10.1128/JVI.02588-06.
86. Leaman DP, Kinkead H, Zwick MB. 2010. In-solution virus capture assay helps deconstruct heterogeneous antibody recognition of human immunodeficiency virus type 1. J Virol 84:3382–3395. https://doi.org/10.1128/JVI.02363-09.
87. Huang CC, Tang M, Zhang MY, Majeed S, Montabana E, Stanfield RL, Dimitrov DS, Korber B, Sodroski J, Wilson IA, Wyatt R, Kwong PD. 2005. Structure of a V3-containing HIV-1 gp120 core. Science 310:1025–1028. https://doi.org/10.1126/science.1118398.
88. Finzi A, Xiang SH, Pacheco B, Wang L, Haight J, Kassa A, Danek B, Pancera M, Kwong PD, Sodroski J. 2010. Topological layers in the HIV-1 gp120 inner domain regulate gp41 interaction and CD4-triggered conformational transitions. Mol Cell 37:656–667. https://doi.org/10.1016/j.molcel.2010.02.012.
89. Hoffenberg S, Powell R, Carpov A, Wagner D, Wilson A, Kosakovsky Pond S, Lindsay R, Arendt H, Destefano J, Phogat S, Poignard P, Fling SP, Simek M, Labranche C, Montefiori D, Wrin T, Phung P, Burton D, Koff W, King CR, Parks CL, Caulfield MJ. 2013. Identification of an HIV-1 clade A envelope that exhibits broad antigenicity and neutralization sensitivity and elicits antibodies targeting three distinct epitopes. J Virol 87:5372–5383. https://doi.org/10.1128/JVI.02827-12.
90. Salomon A, Krachmarov C, Lai Z, Honnen W, Zingman BS, Sarlo J, Gorny MK, Zolla-Pazner S, Robinson JE, Pinter A. 2014. Specific sequences commonly found in the V3 domain of HIV-1 subtype C isolates affect the overall conformation of native Env and induce a neutralization-resistant phenotype independent of V1/V2 masking. Virology 448:363–374. https://doi.org/10.1016/j.virol.2013.10.007.
91. Dey AK, David KB, Ray N, Ketas TJ, Klasse PJ, Doms RW, Moore JP. 2008. N-terminal substitutions in HIV-1 gp41 reduce the expression of nontrimeric envelope glycoproteins on the virus. Virology 372:187–200. https://doi.org/10.1016/j.virol.2007.10.018.